Article

Cell Host & Microbe

Vesicle-Cloaked Virus Clusters Are Optimal Units for Inter-organismal Viral Transmission

Graphical Abstract

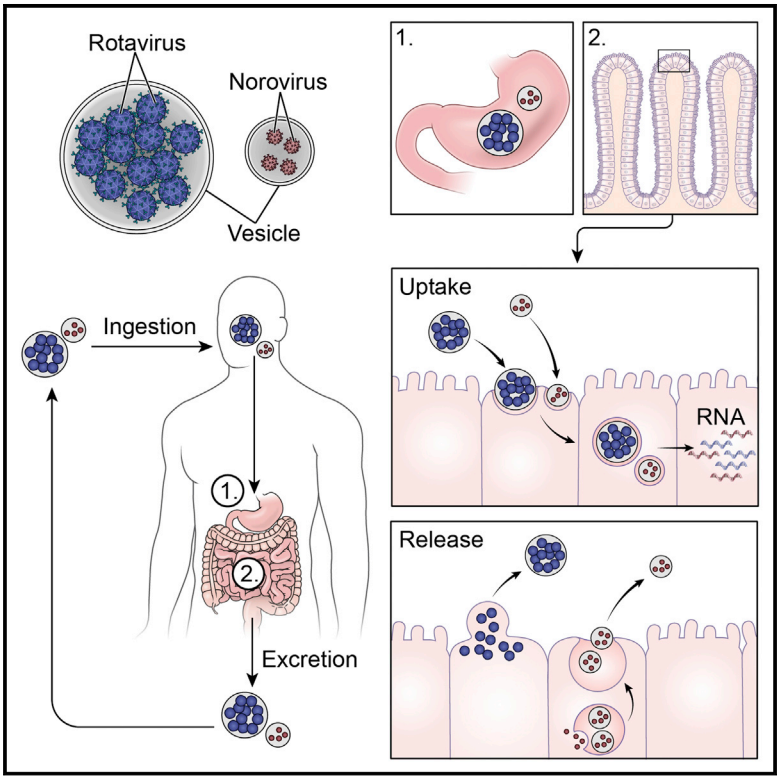

Authors

Marianita Santiana, Sourish Ghosh, Brian A. Ho, ..., Angela Corcelli, Kim Y. Green, Nihal Altan-Bonnet

Correspondence

nihal.altan-bonnet@nih.gov

In Brief

Freely disseminating standalone viral particles are considered the optimal agents for spreading infection. Santiana et al. discover that enteric viruses are also shed in feces as viral clusters cloaked in vesicles. These virus-containing vesicles are a more potent infectious form that enhances the MOI and disease severity.

Highlights

- Rotaviruses and noroviruses are shed in stool as viral clusters inside vesicles
- Vesicles containing virus clusters remain intact during fecal-oral transmission
- Vesicles achieve a high MOI and induce severe disease
- Vesicle-cloaked viral clusters are more virulent units than free viral particles

Santiana et al., 2018, Cell Host & Microbe *24*, 208–220
August 8, 2018
https://doi.org/10.1016/j.chom.2018.07.006

CellPress

CellPress

Cell Host & Microbe
Article

Vesicle-Cloaked Virus Clusters Are Optimal Units for Inter-organismal Viral Transmission

Marianita Santiana,[1,10] Sourish Ghosh,[1,10] Brian A. Ho,[1] Vignesh Rajasekaran,[1] Wen-Li Du,[1] Yael Mutsafi,[1] Dennise A. De Jésus-Diaz,[2] Stanislav V. Sosnovtsev,[2] Eric A. Levenson,[2] Gabriel I. Parra,[3] Peter M. Takvorian,[4,5] Ann Cali,[4] Christopher Bleck,[6] Anastasia N. Vlasova,[7] Linda J. Saif,[7] John T. Patton,[8] Patrizia Lopalco,[9] Angela Corcelli,[9] Kim Y. Green,[2] and Nihal Altan-Bonnet[1,11,*]

[1]Laboratory of Host-Pathogen Dynamics, National Heart Lung and Blood Institute, National Institutes of Health, Bethesda, MD, USA
[2]Laboratory of Infectious Diseases, National Institute of Allergy and Infectious Diseases, National Institutes of Health, Bethesda, MD, USA
[3]U.S. Food and Drug Administration, Division of Viral Products, Silver Spring, MD, USA
[4]Federated Department of Biological Sciences, Rutgers University, Newark, NJ, USA
[5]Albert Einstein College of Medicine, Department of Pathology, Bronx, NY, USA
[6]Electron Microscopy Core, National Heart Lung and Blood Institute, National Institutes of Health, Bethesda, MD, USA
[7]Food Animal Health Research Program, Ohio Agricultural Research and Development Center, CFAES, Veterinary Preventive Medicine Department, College of Veterinary Medicine, The Ohio State University, Wooster, OH, USA
[8]Department of Biology, Indiana University Bloomington, Bloomington, IN, USA
[9]Department of Basic Medical Sciences, Neurosciences and Sensory Organs, University of Bari A Moro, Bari, Italy
[10]These authors contributed equally
[11]Lead Contact
*Correspondence: nihal.altan-bonnet@nih.gov
https://doi.org/10.1016/j.chom.2018.07.006

SUMMARY

In enteric viral infections, such as those with rotavirus and norovirus, individual viral particles shed in stool are considered the optimal units of fecal-oral transmission. We reveal that rotaviruses and noroviruses are also shed in stool as viral clusters enclosed within vesicles that deliver a high inoculum to the receiving host. Cultured cells non-lytically release rotaviruses and noroviruses inside extracellular vesicles. In addition, stools of infected hosts contain norovirus and rotavirus within vesicles of exosomal or plasma membrane origin. These vesicles remain intact during fecal-oral transmission and thereby transport multiple viral particles collectively to the next host, enhancing both the MOI and disease severity. Vesicle-cloaked viruses are non-negligible populations in stool and have a disproportionately larger contribution to infectivity than free viruses. Our findings indicate that vesicle-cloaked viruses are highly virulent units of fecal-oral transmission and highlight a need for antivirals targeting vesicles and virus clustering.

INTRODUCTION

Standalone viral particles have been historically accepted as the optimal infectious units for viral transmission. Indeed, viral particles, moving as independent units, can spread to and infect many more hosts compared with viruses traveling in clusters. In addition, newly replicated viruses, when they are released from cells, have been largely assumed to be genetically homogeneous, with no virus necessarily greater or less infectious than its cohorts. Consequently, infection by one or few independently traveling viral particles has been thought to be generally sufficient for successful transmission. This model of viral transmission has been buoyed by images of freely dispersed viral particles in bodily secretions including stool, saliva, aerosol, etc., as well as by popular methods in virology such as plaque assays which assume the original infecting agents to be free viral particles.

Several recent findings, however, have begun to challenge this "free independent virus particle" view of transmission. Firstly, the viral progeny at the end of an infection cycle, in particular for RNA viruses whose polymerases lack proofreading mechanisms, are rarely identical copies of one another; instead, they are so-called quasispecies (Andino and Domingo, 2015). Practically, this implies that any single member of the progeny cannot be assumed to carry out a successful replication cycle in the next host as it may have attenuating mutations.

Secondly, enteroviruses including poliovirus, Coxsackievirus, and rhinovirus have all been found to transmit themselves *in vitro* as viral clusters inside extracellular vesicles (EVs) (Altan-Bonnet, 2016; Chen et al., 2015; Bird et al., 2014; Robinson et al., 2014). The infection pathway by these vesicles begins with their internalization within endocytic compartments of susceptible cells, followed by their vesicle membranes becoming disrupted through not yet entirely known mechanisms (Feng et al., 2013; Yin et al., 2016), and followed by the enteroviruses binding their receptors from within the endocytic compartment and transferring multiple viral genomes simultaneously into the cytosol of the host cell (Chen et al., 2015). Significantly, inoculation of a culture of cells with clustered enteroviruses inside vesicles yields far greater amounts of virus production than when a similar culture of cells has been inoculated with *equivalent amounts of freely disseminating* enterovirus particles (Chen et al., 2015). This finding suggests that there are replication

barriers to viruses when they enter cells as single particles or in low numbers (Chen et al., 2015; Altan-Bonnet, 2016; Diaz-Munoz et al., 2017). These barriers may be manifold and include mutations that impact viral genome structure and expression of viral enzymes, inefficient translation and/or replication reactions due to low levels of viral proteins being generated at the start of infection, and more effective host defenses being able to be mounted against fewer entering genomes (Altan-Bonnet, 2016; Diaz-Munoz et al., 2017). In contrast, when viruses can enter cells simultaneously in multiple copies, such as by being clustered inside vesicles (Chen et al., 2015) or on the surface of bacteria (Erickson et al., 2018), or even as free particles, but inoculated at high concentrations (Bordería et al., 2015), they can produce a rapid rise in viral replication protein levels as well as increase their probability of engaging in cooperative and complementary interactions among themselves (e.g., sharing genomes or replication machinery). Indeed, in such cases *in vitro*, a higher recombination rate and greater genetic diversity have been observed (Bordería et al., 2015; Erickson et al., 2018).

Whether a collective mode of transmission exists *in vivo* and delivers any advantages to viruses has not yet been tested. Here, we demonstrate that rotaviruses and noroviruses, two non-enveloped RNA viruses that are the major causes of mortality and morbidity associated with severe gastrointestinal (GI) infections (Ramani et al., 2014; Greenberg and Estes, 2009; Karst et al., 2014), are transmitted in stool as clusters of viruses inside vesicles. We show that vesicles containing rotavirus can be transmitted through stools among animals through the fecal-oral route, and these vesicles remain intact as they pass through the GI tracts to deliver multiple viral particles simultaneously to target cells in the intestines of the animals. This mode of transmission results in far greater levels of intestinal infection and significantly more severe clinical signs than when animals ingest equivalent amounts of free viruses. Notably, we find that vesicle-cloaked viruses have a disproportionately *larger* contribution to the infectivity of stool than that of free virus particles. Our findings indicate that vesicle-cloaked virus clusters are highly pathogenic units of stool and highlight a need for antivirals targeting vesicles and virus clustering.

RESULTS

In Vitro, Rotaviruses Are Released Entirely Non-lytically within EVs

We began our studies on the role of vesicles in inter-host transmission by focusing on rotavirus spread, for which multiple animal model systems exist closely replicating rotavirus fecal-oral transmission, tissue tropism, and clinical signs (Greenberg and Estes, 2009). To date, cell lysis and dissemination as naked non-enveloped virus particles have been accepted as the mode of rotavirus transmission. Given this, we first set out to determine how rotavirus egressed from cells *in vitro*. H69 human cholangiocytes (Coots et al., 2012) were infected with rotavirus *SA11* at high enough multiplicity such that ~70% of the cells had been infected at the time of inoculation (Figure S1A). Changes in plasma membrane permeability to trypan blue dye were monitored as a function of rotavirus release (Chen et al., 2015), the latter quantified by ELISA. All raw ELISA readings are presented in the Supplemental Tables. Remarkably, there was no significant change in cell permeability for up to 72 hr post-inoculation (hpi), while ~100% of the total releasable rotavirus pool exited the cells (Figure 1A; Table S1). Examination of another cell line, MA104 infected with *SA11*, also revealed a fraction of the virus to be released before membrane lysis (Figures S2A and S2B). These data indicated that rotavirus did not need cell lysis to exit and that cell lysis was likely a cell-type-dependent response to rotavirus infection.

We next asked how rotavirus was able to non-lytically exit cells. It is widely accepted that rotavirus genomes replicate and assemble into double-layered particles (DLPs), comprised of inner and intermediate capsid proteins (VP1, VP2, VP3, and VP6) within the cytoplasm of host cells (Trask et al., 2012). The subsequent stages which culminate in the formation of triple-layered non-enveloped particles (TLPs) are mostly unknown but are thought to involve the DLPs budding into the ER and picking up the ER membrane-associated final outer capsid proteins VP4 and VP7. The ER lipids are then removed from the particles concurrent with the condensation of VP4 and VP7 onto the DLPs before the particles get out of the ER and cell by lysis (Trask et al., 2012). H69 cells at 24 hpi were fixed and immunostained with antibodies against VP6 and a commercial neutralizing antibody that we found recognized assembled TLPs (Figure S1B). Confocal imaging revealed that TLPs and VP6 were co-localized to areas beneath the plasma membrane and within plasma membrane protrusions (Figure 1B). These protrusions could be labeled with membrane selective CellBrite Fix 488 fluorescent dye (Figure 1C) and were also observed at the surface of MA104 cells prior to lysis (Figures 1D and 1E).

Given the above, we investigated if rotavirus was being released non-lytically through EVs potentially derived from the plasma membrane. As nearly all forms of EVs contain membranes with inverted phosphatidylserine (PS) lipid topology (Chen et al., 2015; Haraszti et al., 2016; van Niel et al., 2018), EVs can be isolated by pull-down with PS-binding proteins Annexin V or TIM4 coupled to magnetic beads (Miyanishi et al., 2007; Chen et al., 2015). Applying this strategy to the extracellular media collected from infected H69 and MA104 cell cultures, we found that rotavirus particles were enriched in EVs (van Niel et al., 2018) sedimenting at 10,000 × *g* (Figures 1F and S2C; Table S1). Note that the PS-binding proteins did not themselves bind free (naked) rotavirus nucleocapsids (Figure S1C). Negative-stain electron microscopy of bead eluates from MA104 cells confirmed the presence of large vesicles, each carrying multiple rotavirus particles (Figure S2D).

Consistent with a plasma membrane origin, we found that EVs were enriched in plasma membrane protein CD98 and lipids including PS, phosphatidylethanolamine (PE), and sphingomyelin (SM) (Figures 1G and S2E). Notably, EVs lacked Sec61β, an otherwise abundant ER membrane protein (Figure 1G), arguing against vesicles being a product of indiscriminate cell blebbing. Furthermore, the EVs were unlikely to be exosomes, which are small vesicles (<200 nm diameter) that are the product of the fusion of multivesicular bodies (MVBs) with the plasma membrane (Kowal et al., 2014) since they were sedimenting at 10,000 × *g*, indicating a diameter >200 nm (Haraszti et al., 2016) (Figure 1F), and were devoid of CD63 (Figure 1G), a protein

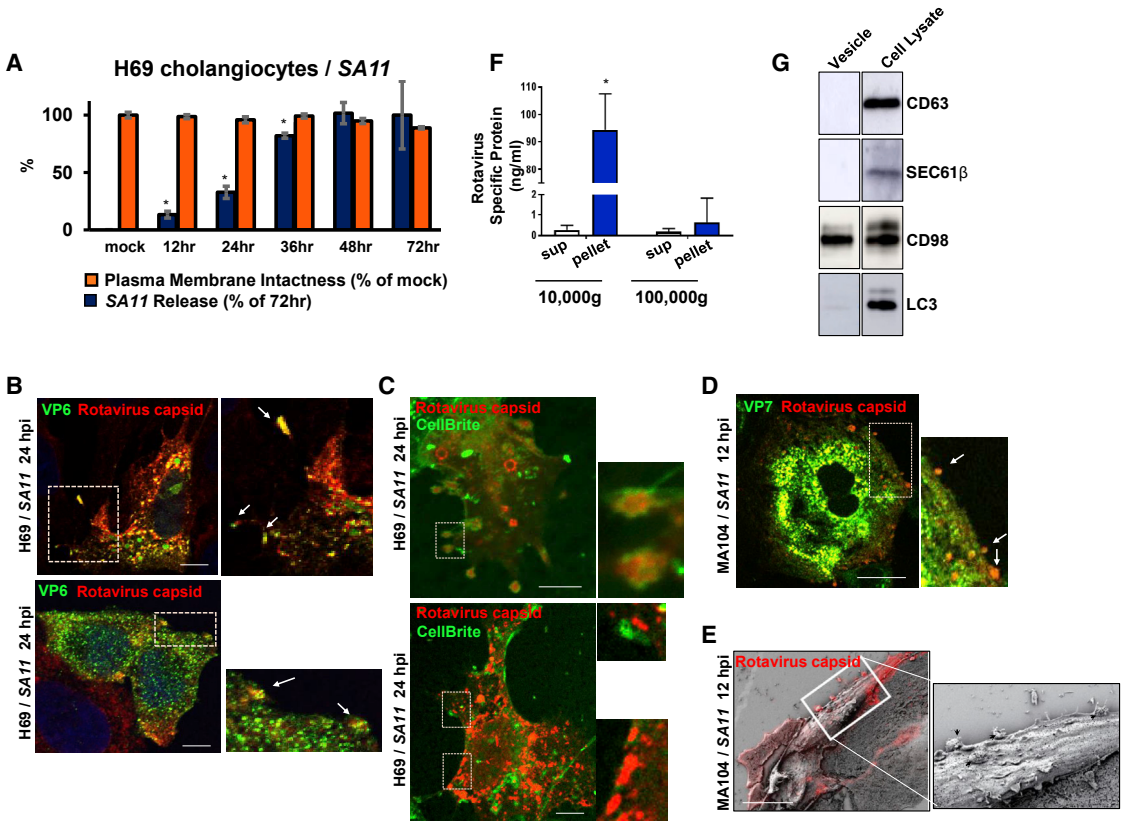

Figure 1. Rotaviruses Exit Cells Non-lytically Inside Large Extracellular Vesicles

(A) Non-lytic release of rotavirus from cells. H69 cell plasma membrane intactness during virus release from cells infected with *SA11* rotavirus was monitored and plotted. Amount of virus released was determined by ELISA and normalized to the total releasable pool of virus at 72 hpi. Error bars are SD from three independent experiments (*$p < 0.05$). See Table S1 for raw ELISA data.

(B) Subcellular rotavirus distribution in H69 cells at 24 hpi with antibodies against capsid subunit VP6 and rotavirus nucleocapsids (Figure S1B). Arrows point to cell surface protrusions containing rotavirus nucleocapsids. Scale bars, 5 μm.

(C) Plasma membrane protrusions from H69 cells contain rotavirus nucleocapsids. Cells were immunostained with anti-rotavirus nucleocapsid antibody and counterstained with CellBrite Fix 488 fluorescent membrane dye. Scale bars, 5 μm.

(D) MA104 cells at 12 hpi were fixed and immunostained with antibodies against VP7 and rotavirus nucleocapsids. Arrows point to cell surface protrusions containing rotavirus nucleocapsids. Scale bar, 5 μm.

(E) MA104 surface protrusions containing rotavirus nucleocapsids can be visualized by correlative light electron microscopy with antibodies against the assembled rotavirus capsids. Scale bar, 5 μm.

(F) Rotaviruses released from H69 cells are associated with large PS vesicles. Cell culture medium from infected H69 cells was subjected to differential centrifugation. Supernatant and pellet fractions were incubated with Annexin V-coupled (ANX) magnetic beads. Eluates were analyzed by ELISA. The values represented in the bar graph represent the mean value from two independent experiments, error bars are SD (*$p < 0.05$). See Table S1 for raw ELISA data.

(G) CD98, LC3, CD63, and SEC61β distribution in vesicles isolated at 48 hpi from the culture medium of infected H69 cells. Samples were subjected to SDS-PAGE/western analysis with relevant antibodies and levels of proteins were compared with infected H69 cell lysates.

typically enriched in MVBs. In addition, intracellular rotaviruses never co-localized with MVBs (Figure S1D) and EV production was not impacted by GW4869, an inhibitor of exosome release (Urbanelli et al., 2013) (Figure S2F). The vesicles also did not contain any significant levels of LC3 (Figure 1G), a marker for EVs derived from secretory autophagosomes (Chen et al., 2015), and rotavirus nucleocapsids and LC3 were never co-localized intracellularly (Figure S1E). Together these data suggest that rotaviruses egress from cells non-lytically in large EVs that are derived from the plasma membrane. These types of large EVs have also been termed "microvesicles" (Gould and Raposo, 2013). Notably blue tongue virus, a close relative of rotavirus, can also egress from the plasma membrane in vesicles (Mohl and Roy, 2014).

Vesicle-Contained Rotaviruses in Animal Stools

Freely dispersed rotavirus virions are frequently observed in electron micrographs of infected stools (Trask et al., 2012). Given our findings above, we set out to determine whether rotavirus-containing EVs also existed within stool. Gnotobiotic piglets and BALB/c suckling mouse pups were inoculated orally with human rotavirus *Wa* strain and murine EDIM (epizootic diarrhea of infant mice) strain, respectively. Stools were collected at peak virus shedding, 2 days post-infection (dpi), and incubated with Annexin V- or TIM4-coupled magnetic beads to isolate putative rotavirus-containing vesicles. Magnetic isolation followed by SDS-PAGE/western analysis of the bead eluates revealed rotavirus nucleocapsid proteins VP6 and VP7 to be associated with PS membranes within the pig and mouse stools (Figures 2A and 2B).

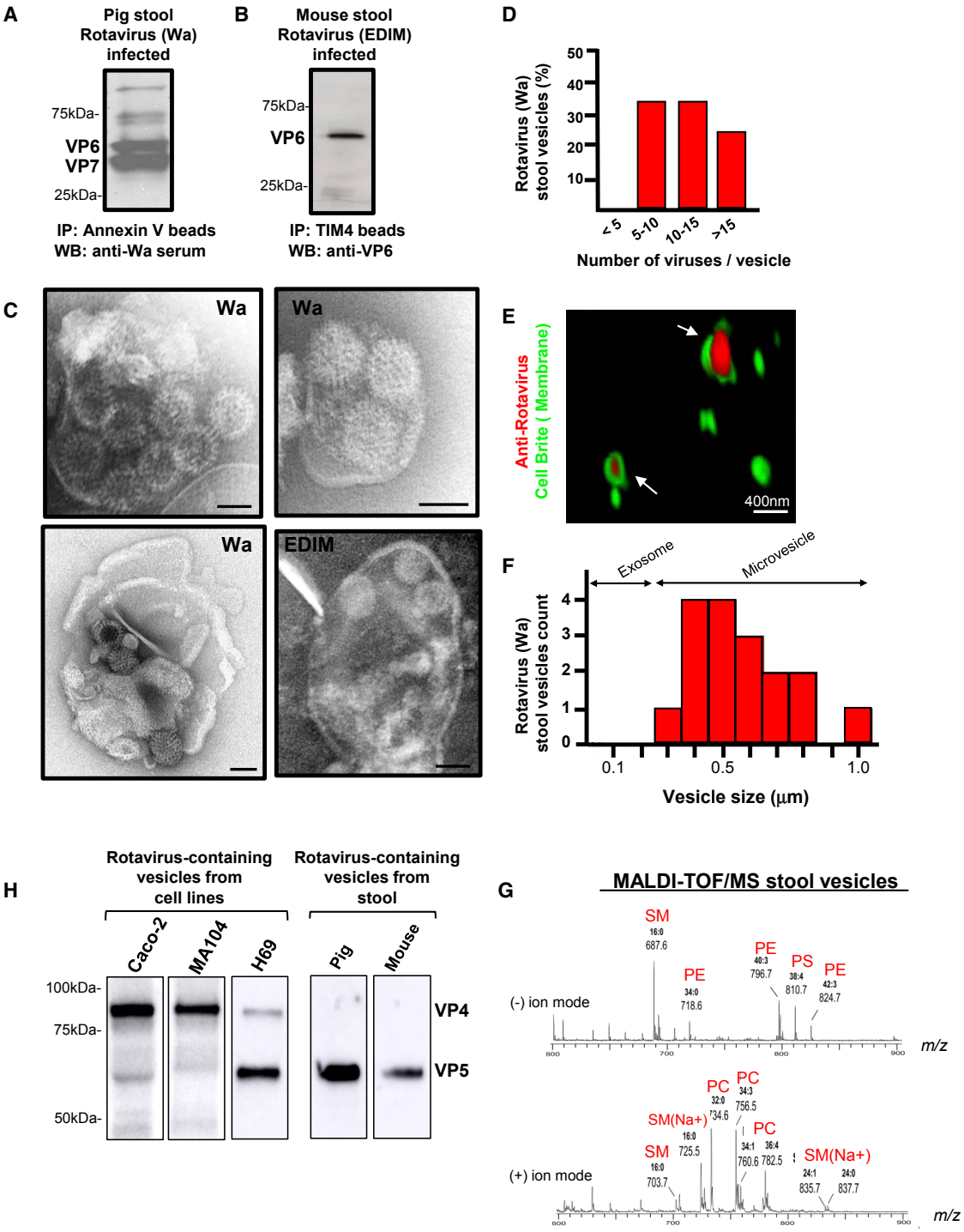

Figure 2. Infectious Rotavirus-Containing Large EVs Are Found Shed in Stool

(A and B) Rotavirus capsid subunits are associated with PS vesicles isolated from the stools of gnotobiotic pigs and mouse pups previously infected with Wa or EDIM rotavirus strains, respectively. Stool vesicles isolated with Annexin V- or TIM4-coupled magnetic beads were eluted and subjected to SDS-PAGE/western analysis with either polyclonal serum against human rotavirus strain Wa (A) or anti-EDIM VP6 antibody (B).

(C) Negative-stain electron microscopy was performed on the bead eluates from (A) and (B). Scale bars, 70 nm.

(D) The number of particles carried by individual Wa-containing vesicles was determined from negatively stained electron micrographs. A total of 25 vesicles were analyzed.

(E) Structured illumination microscopy performed on Wa-containing vesicles co-stained with CellBrite Fix 488 fluorescent membrane dye and antibodies against rotavirus nucleocapsids. Arrows point to the dual-labeled vesicles. Scale bar, 400 nm.

(legend continued on next page)

Stool Vesicles Transport Clusters of Rotavirus Particles

To verify that the capsid proteins pulled down from stool were rotavirus particles *inside* PS vesicles, we performed negative-stain electron microscopy. Numerous vesicles, each loaded with multiple rotavirus particles, were observed in both the pig and mouse stool samples (Figure 2C), with >60% of rotavirus-containing EVs having more than ten particles per vesicle (Figure 2D). Super-resolution imaging of the stool vesicles labeled with CellBrite Fix 488 fluorescent membrane dye and anti-rotavirus antibodies also confirmed the viruses to be inside the EVs, with 70% of the EVs consisting of microvesicles >500 nm in diameter (Figures 2E and 2F).

MALDI-TOF/mass spectrometry (MS) lipid analysis of stool vesicles revealed enrichment of plasma membrane lipids including SM, PE, and PS (Figure 2G). Rotaviruses replicate in enterocytes (Greenberg and Estes, 2009) and, while other cell/organelle sources cannot be completely ruled out, our findings, including size and lipid composition, are consistent with rotavirus-containing stool EVs being produced from enterocyte microvilli plasma membranes. Note that the latter is a well-known generator of EVs (McConnell et al., 2009).

Stool Vesicles Contain Activated Infectious Rotaviruses

The VP4 nucleocapsid protein of the TLP must be proteolytically cleaved into VP5 and VP8 for rotaviruses to be activated and infectious (Crawford et al., 2001). As stool rotaviruses had previously been assumed to exist only as free particles (i.e., unenclosed by membrane), this cleavage was thought to be easily catalyzed by stool or GI tract proteases. Given this, we investigated the state of VP4 on rotaviruses enclosed inside EVs. Surprisingly, we found that the VP4 of rotaviruses inside isolated stool vesicles were already in their cleaved and activated state, as indicated by the presence of VP5 (Figure 2H). Moreover, while the EVs collected from the culture medium of infected MA104 or Caco-2 cells still contained rotaviruses with uncleaved VP4 (Figure 2H), the EVs collected from infected H69 cell cultures contained activated, VP4-cleaved rotaviruses (Figure 2H). These findings indicate that *in vivo* (and *in vitro* with H69 cells), rotaviruses are shed as membrane-cloaked clusters of activated infectious viruses, with proteolytic cleavage likely taking place either just prior to or after packaging into EVs.

Noroviruses Are Shed in Stool Inside Exosomes

We next asked whether other enteric viruses might be shed into stool inside EVs. Norovirus replicates in the intestinal tract and also spreads by fecal-oral transmission (Kapikian et al., 1972; Karst et al., 2014; Wobus et al., 2006). Stool samples from multiple different infected patients were collected and incubated with TIM4-coupled beads. Analysis of the bead eluates indicated the presence of human norovirus capsid protein VP1 to be associated with PS vesicles (Figure 3A). Note that TIM4 did not bind naked norovirus particles (Figure S3A). Electron microscopy of the eluates revealed numerous small vesicles (Figure 3B), ~90% with diameter <200 nm and carrying between 1 and 5 virus particles/vesicle (of n = 25 vesicles counted). Their small size suggested they were MVB-derived exosomes (Kowal et al., 2014) and, consistent with this, they could be isolated from human stools with antibodies against CD63, CD9, and CD81 (Figure S3B), all proteins known to be enriched in MVB-derived exosomes.

The data above suggested that human norovirus is shed non-lytically into stools inside exosomes derived from infected host tissues. To investigate this further, we measured the plasma membrane permeability of RAW264.7 cells in culture during infection with a rodent norovirus homolog, murine norovirus-1 (MNV-1). We found that ~100% of the total releasable MNV-1 pool egressed from these cells non-lytically (Figure 3C). Similar to human norovirus, extracellular MNV-1 was enriched in exosome-like small PS vesicles, which sedimented at 100,000 × *g* and contained fewer than 5 virus particles per vesicle (Figures 3D and 3E). Consistent with these MNV-1 containing vesicles being MVB-derived exosomes, extracellular levels of MNV-1 were reduced by acute GW4869 treatment (Figure 3F) while replication was unaffected (Figure S3C), and MALDI-TOF/MS lipid analysis of the vesicles revealed the presence of bis(monoacylglycero)phosphate (BMP) (Figure 3G), a lipid enriched in MVBs and MVB-derived exosomes (Skotland et al., 2017).

We then tested whether the exosomes containing noroviruses (human or MNV-1) were infectious. Human enteroid cultures (Ettayebi et al., 2016) and RAW264.7 cell cultures were inoculated with human norovirus or MNV-1-containing exosomes, respectively (Figures 3H and 3I). A significant 2-log increase in human norovirus genome copy numbers within 93 hr of washing the vesicle inoculum off the enteroids was measured, indicating that the human norovirus-containing exosomes isolated from stools were infectious (Figure 3H). MNV-1-containing exosomes isolated from cell culture were also infectious when inoculated into new RAW264.7 cells (Figure 3I, vesicle).

Notably, the infectivity of the MNV-1-containing exosomes was still dependent on the MNV-1 receptor, CD300lf, being expressed on cells (Orchard et al., 2016): blocking the receptor with antibodies *prior* to inoculation completely inhibited infection (Figure 3I, anti-CD300lf). This ruled out a simple vesicle membrane-host plasma membrane fusion as the mode virus delivery into the host. Moreover, inoculation with CellBrite Fix 488-labeled fluorescent MNV-1 exosomes followed by confocal z-sectioning revealed an ~50% decrease in exosome uptake in cells pre-treated with anti-CD300lf antibodies relative to cells pre-treated with immunoglobulin G (IgG) (Figures 3J and 3K). It is worth noting that CD300lf is a member of a family of PS receptors (Borrego, 2013). Our findings suggest a possible dual role for CD300lf in mediating MNV-1 infection: first enabling exosome internalization into an endocytic compartment through

(F) Vesicle size distribution obtained from the structured illumination images of vesicles in (E). Of the 17 vesicles that were analyzed, ~70% were of diameter >500 nm. This indicates that rotavirus-containing vesicles, in terms of size, largely fall into the category of microvesicles rather than the smaller exosomes.
(G) MALDI-TOF/MS analyses of EDIM rotavirus-containing vesicles isolated from mouse stools.
(H) VP4 cleavage analysis of rotaviruses inside vesicles isolated from pig and mouse stools; and *SA11*-infected H69, Caco2, and MA104 cell culture media. Samples were subjected to SDS-PAGE/western analysis with anti-VP5 antibody.

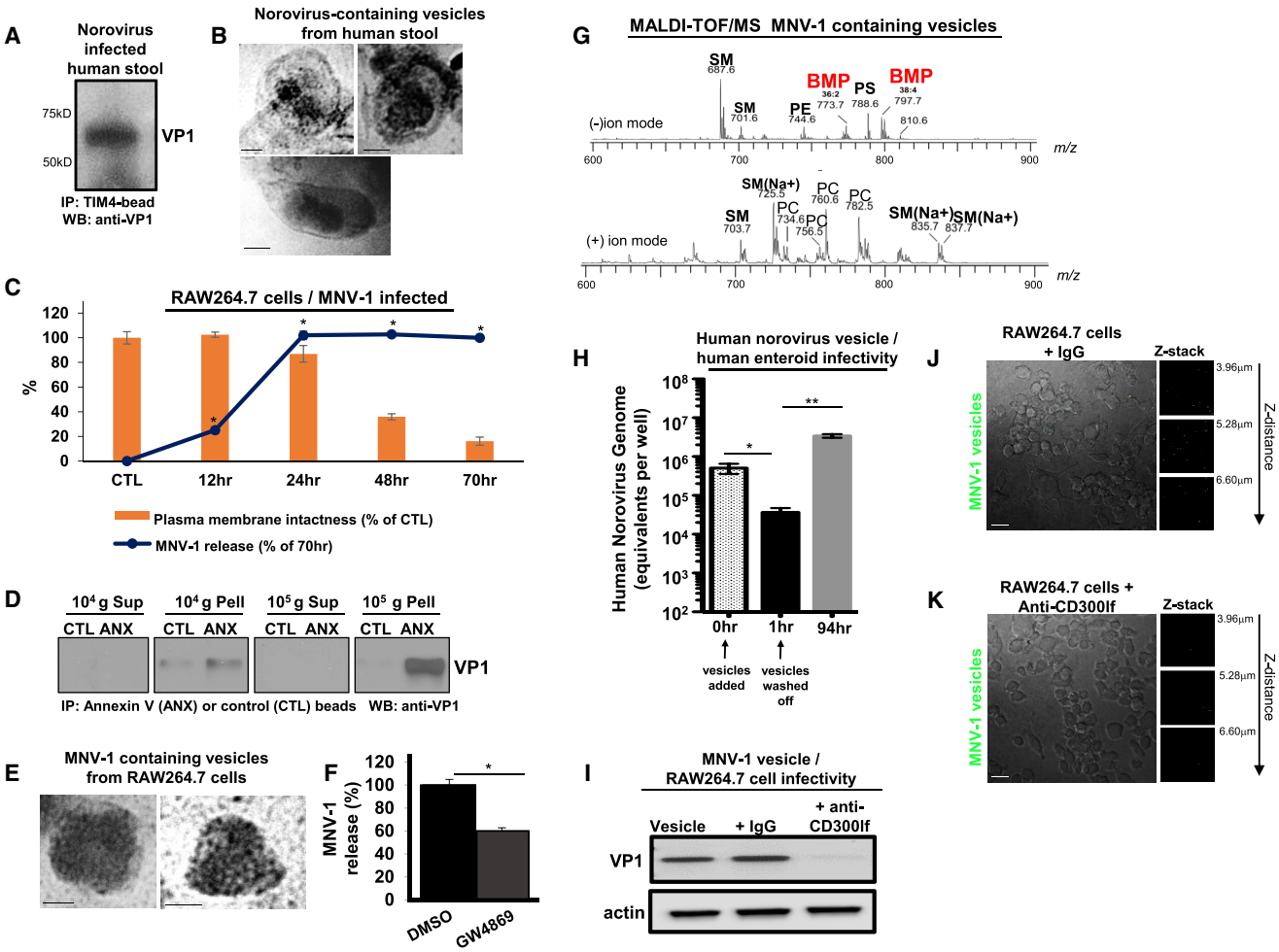

Figure 3. Infectious Human and Murine Noroviruses Are Shed in Stool in Exosomes

(A) Stool collected from norovirus-infected patients was incubated with TIM4-coupled magnetic beads and eluates subjected to SDS-PAGE/western analysis with anti-human norovirus VP1 antibody. Representative result from one patient's stool is presented here; see Figure S3B for results from other infected human stool samples where isolation was performed with antibodies against exosome proteins CD63, CD81, and CD9.

(B) Negative-stain electron micrographs of TIM4 bead eluates from (A) reveal small exosome size (<200nm) vesicles containing norovirus particles. Scale bars, 30 nm.

(C) Non-lytic murine norovirus (MNV-1) release from RAW264.7 cells. Plasma membrane intactness relative to virus released was monitored and plotted. Amount of virus released was determined by qRT-PCR and normalized to the total releasable pool of virus at 70 hr pi. Error bars are SD from three independent experiments (*$p < 0.02$).

(D) Extracellular MNV-1 is associated with small exosome size PS-enriched vesicles sedimenting at 100,000 × *g*. Cell culture medium from mock and infected RAW264.7cells was subjected to differential centrifugation; both supernatant and pellet fractions were incubated with Annexin V-coupled (ANX) or control (CTL) magnetic beads. Eluates were subjected to SDS-PAGE/western analysis with anti-murine norovirus VP1 antibody.

(E) Negative-stain electron micrographs of Annexin V bead eluates from the 100,000 × *g* pellet in (D) reveal small exosome-size vesicles containing MNV-1 particles. Scale bars, 30 nm.

(F) MNV-1 release is sensitive to GW4869, suggesting that the vesicles are exosomes derived from MVBs. Error bars are SE from two independent experiments (*$p < 0.02$).

(G) MALDI-TOF/MS analyses of MNV-1-containing vesicles isolated from RAW264.7 cell culture reveal the presence of an MVB/exosome lipid, BMP.

(H) Human intestinal enteroid cultures were inoculated with exosomes previously isolated from a norovirus-infected human stool. After 1 hr, the culture was washed and incubated for another 93 hr. Norovirus RNA was extracted at the indicated times and quantified by qRT-PCR. Error bars are SE from triplicate readings from three experimental wells (*$p < 0.0001$; **$p < 0.0003$).

(I) MNV-1-containing exosomes require CD300lf for infectivity. RAW264.7 cells were pre-treated with IgG (mock) or anti-CD300lf antibodies prior to inoculation with MNV- containing exosomes. Cell lysates were collected at 12 hpi and subjected to SDS-PAGE/western analysis with anti-VP1 antibody.

(J and K) MNV-1 exosomes require CD300lf for internalization into cells. RAW264.7 cells were treated as in (I), but cells were inoculated with CellBrite Fix 488-labeled MNV-1-containing vesicles for 30 min. Confocal z stacks (0.2 μm/slice) of fields of cells were obtained. Representative fields (phase/fluorescence combined) and a subset of their corresponding z stacks (only fluorescence) are presented. Scale bar, 10 μm. 44 cells per field of view were analyzed for each treatment condition. Quantification revealed an average of 2.93 ± 0.23 (SE) vesicles taken up per IgG-treated cell and 1.37 ± 0.43 (SE) vesicles taken up per anti-CD300lf-treated cell.

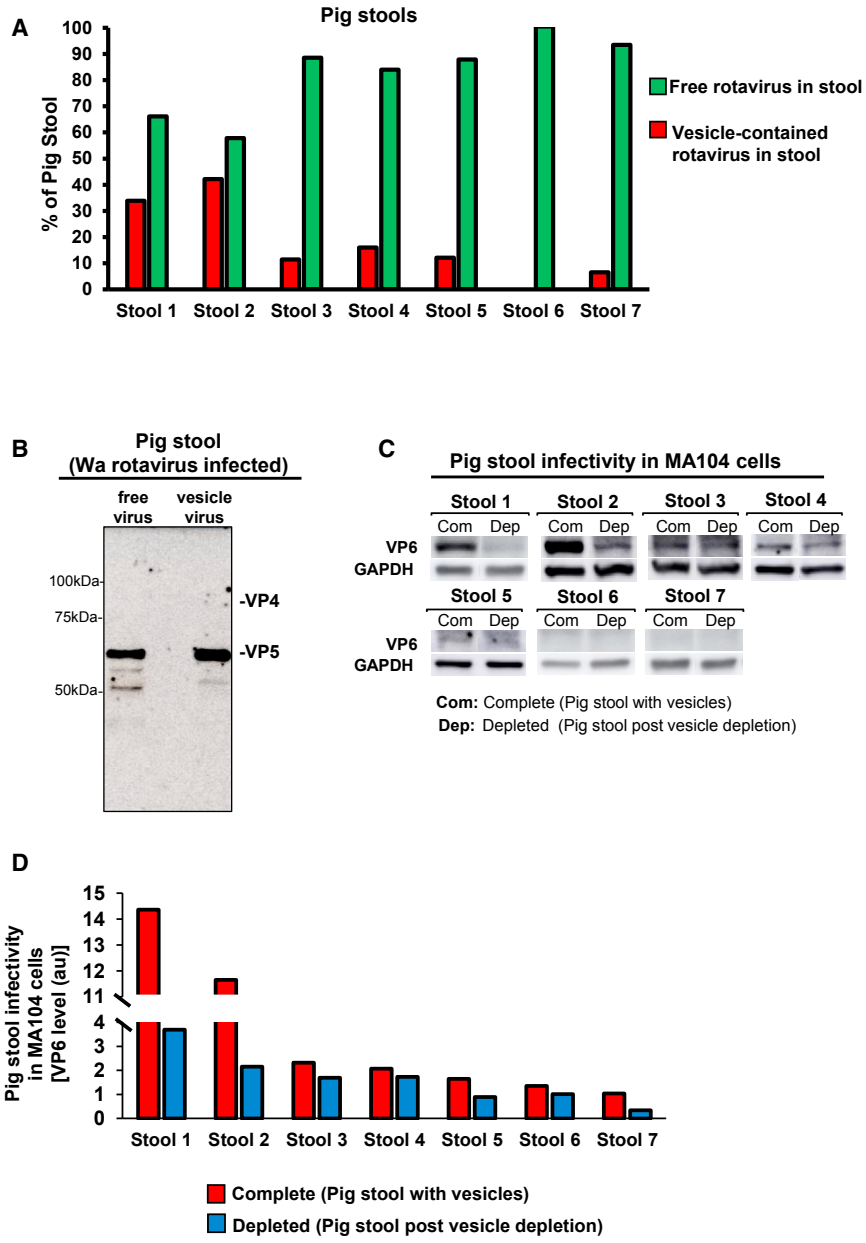

Figure 4. Vesicle-Contained Rotaviruses from Stool Are More Infectious Than Free Stool Rotaviruses *In Vitro*

(A) Quantification by ELISA of vesicle-contained and free rotavirus pools in stools obtained from seven infected gnotobiotic pigs. Data were plotted as percentages of the total rotavirus pools in each stool sample. See Table S2 for raw ELISA data.

(B) VP4 cleavage state of stool rotaviruses inside and outside the vesicles. Free stool rotaviruses were immuno-precipitated with anti-rotavirus nucleocapsid antibody (GTX 39230); vesicle-contained rotaviruses were isolated with TIM4-coupled beads. Samples were subjected to SDS-PAGE/western analysis with anti-VP5 antibody.

(C and D) Infectivity of rotavirus stools before (Complete) and after (Depleted) vesicle depletion. MA104 cells were inoculated with either complete or depleted stool solutions, and samples were collected at 6 hpi. Cell lysates were subjected to SDS-PAGE/western analysis with anti-rotavirus VP6 antibody (C). Quantification of VP6 protein levels (D); stool numbering matches the sequence from (A).

interaction with vesicle PS lipids; then, subsequent to disruption of the vesicle membrane by lipases within endosomes (Yin et al., 2016), binding to the MNV capsids and mediating genome transfer into the cytosol (Orchard et al., 2016).

Vesicle-Contained Rotaviruses Are a Significant Fraction of the Stool Rotavirus Pool

As we now had established that both rotaviruses and noroviruses could be shed in stool inside EVs, we next determined their contribution to stool infectivity in fecal-oral transmission. Focusing on the robust animal models available for rotavirus fecal-oral transmission for these subsequent studies, we first quantified the relative amounts of free and vesicle-contained rotaviruses within the stools of rotavirus-infected piglets (Figure 4A; Table S2) and mouse pups (Figure 5A; Table S3).

Separate stool samples were collected from seven rotavirus-infected piglets (Figure 4A) and three rotavirus-infected mouse pups (Figure 5A). To quantify the vesicle-contained virus fraction in each stool sample, the stool solutions were centrifuged at 10,000 × *g* to pellet vesicles >200 nm diameter. Both the pellet and supernatant fractions were subjected to multiple rounds of TIM4-coupled bead isolation to remove all vesicle-contained rotaviruses until no more bound to the beads, as assayed by ELISA. The TIM4 isolates from the initial pellet and all the consecutive pull-downs were pooled and referred to as the "vesicle-contained rotavirus." The remaining rotaviruses in the supernatants that did not come down with TIM4 were referred to as "free rotaviruses in stool." Subsequently, aliquots of vesicle-contained and free rotavirus fractions were assayed by ELISA to quantify each of their respective virus pools, with the vesicle aliquots being lysed first to free their virus cargo. The ELISA results were validated by qRT-PCR measurements of viral genomes (Figure S4A). The results in Figures 4A and 5A demonstrate that vesicle-contained rotaviruses constitute a non-negligible fraction, comprising from 10% to 45% of the total stool rotavirus pools.

Vesicle-Contained Rotaviruses from Stool Are More Infectious Than Free Stool Rotaviruses *In Vitro*

We next investigated the contribution of vesicle-contained rotavirus populations to the overall infectivity of the pig stool samples. The VP4 of rotaviruses inside and outside the stool vesicles was in its cleaved state (i.e., VP5 and Vp8), indicating

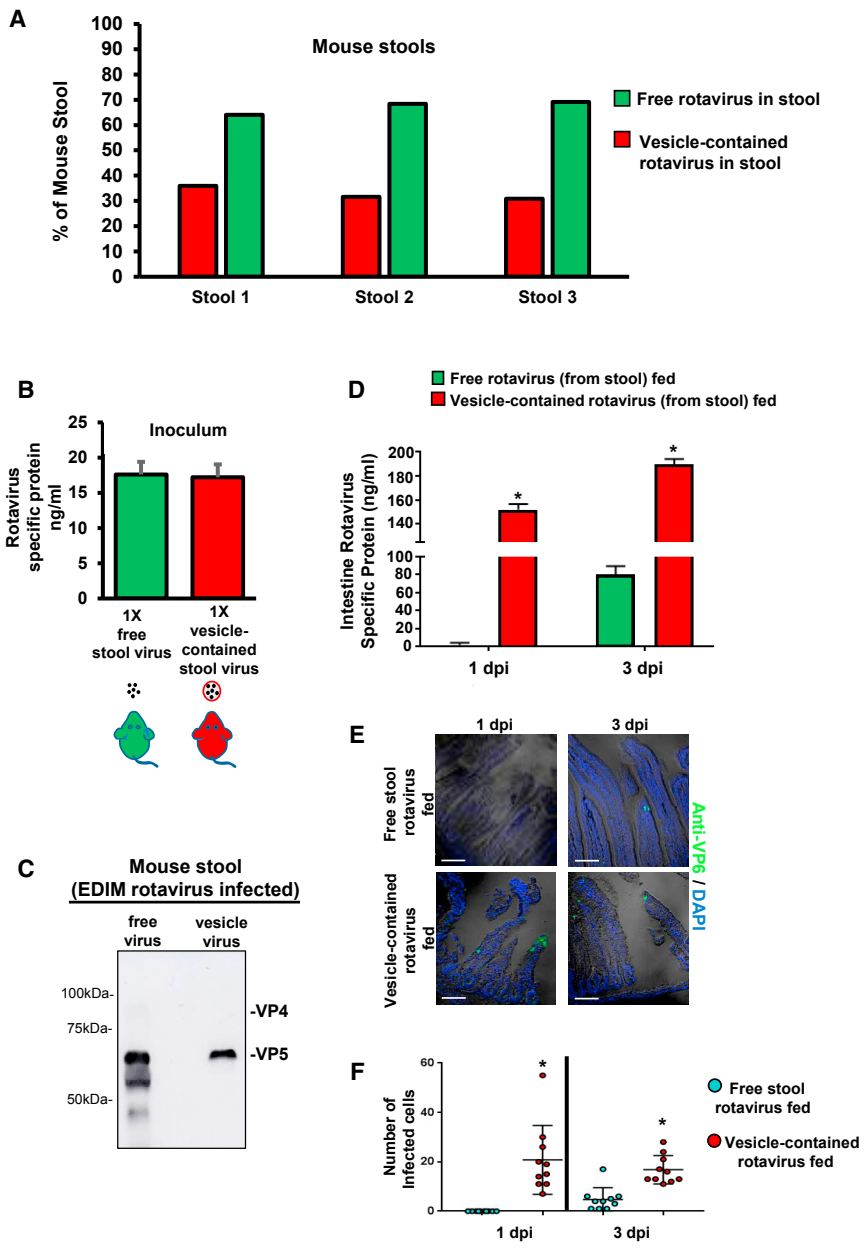

Figure 5. Vesicle-Contained Rotaviruses from Stool Are More Infectious Than Free Stool Rotaviruses *In Vivo*

(A) Quantification by ELISA of vesicle-contained and free rotavirus pools in stools obtained from three infected mouse pups. Data are plotted as percentages of the total rotavirus pools in each stool sample. See Table S3 for raw ELISA data.

(B) Inoculum containing free stool rotavirus (prepared by sequential removal of vesicles from mouse stool) or the intact removed vesicles were titrated using a rotavirus-specific ELISA and adjusted so that equivalent amounts of virus would be fed in each experiment (of two independent experiments). The graph represents the amount of virus that was contained within 25 μL of each inoculum, which was subsequently fed into separate groups of mouse pups (n = 4 pups for each group). Each bar is a representative means calculated from the analyses; error bars are SD. See Table S3 for raw ELISA data.

(C) VP4 cleavage state of stool rotaviruses inside and outside the vesicles. Free mouse stool rotaviruses were immuno-precipitated with anti-rotavirus nucleocapsid antibody (GTX39230); vesicle-contained rotaviruses were isolated with TIM4-coupled beads. Samples were subjected to SDS-PAGE/western analysis with anti-VP5 antibody.

(D) Rotavirus replication within mouse intestines. Intestinal tissues excised from two animals from each inoculated group at 1 and 3 dpi were homogenized and analyzed by ELISA. Each bar in the graph represents the average amount of viral protein corresponding to the sample. Error bars are SD from two animals for each group from two independent experiments (*$p < 0.05$). See Table S3 for raw ELISA data.

(E) Upper small intestinal tissue (duodenum and jejunum) was excised from one animal in each group at 1 and 3 dpi and processed for immunohistochemistry with antibodies against rotavirus capsid (green), and co-stained with DAPI to visualize the nuclei. Panel figures are representative of ten independent areas of the small intestines, corresponding to each group, from two independent experiments. Images captured at 20× magnification. Scale bars, 100 μm.

(F) Quantification of the numbers of infected cells within the small intestines presented in (E). Ten independent areas of the small intestines were analyzed for each group. Each individual data point in the graph represents the total number of cells infected in that particular area of interest per group represented along with SD (*$p < 0.05$).

that both rotavirus pools contained activated viruses (Figure 4B). An aliquot from each rotavirus-infected pig stool sample was split into two fractions of equal volume, where one fraction was unprocessed and referred to as "complete"; the other processed as described above to remove all vesicles and referred to as "depleted." MA104 cells were subsequently inoculated with either complete or vesicle-depleted pig stools and, after 6 hr, VP6 production was measured as an indicator of infectivity and viral replication (Figures 4C, 4D, and S4B). We found that all the complete stools (i.e., containing vesicles) were more infectious than the vesicle-depleted stools (Figure 4D). But, remarkably, the decrease in infectivity of vesicle-depleted pig stools was not proportional with the amounts of vesicle-contained viruses removed from the stool. For example, in pig stools no. 1 and no. 2, the vesicle-contained viruses made up 35% and 42% of the total pool, respectively, but stool infectivity post-vesicle depletion decreased by 72% and 83%, respectively. Furthermore, while the free virus pools of stools no. 3 to no. 7 were in far greater excess to their vesicle-contained virus populations, the overall infectivity of these stools was negligible compared with those of stools no. 1 and no. 2 (Figure 4D). Together, these data suggest that

vesicle-contained rotaviruses are a greater contributor to stool infectivity than free viruses.

Vesicle-Contained Rotaviruses from Stools Are More Infectious Than Free Stool Rotaviruses *In Vivo*

We followed up by investigating whether vesicle-contained rotaviruses were also more infectious than free rotaviruses in fecal-oral transmission among animals. Rotavirus-containing vesicles were collected from mouse stools along with the remainder of the vesicle-depleted stools; each pool was quantified by ELISA and the vesicle-depleted pools adjusted so that their rotavirus levels matched those of the vesicle-contained fractions (Figure 5B; Table S3). Subsequently two groups of suckling mouse pups were fed by oral gavage with equal amounts of rotavirus, with one group receiving the vesicle-contained virus and the other group receiving the free virus left behind in the depleted stools (Figure 5B). Notably, while both pools of rotaviruses were in their activated forms, similar to that observed with the pig stools (Figure 4B), with their VP4 proteins cleaved into VP5 (and VP8) (Figure 5C), the free rotaviruses also had multiple lower bands cross-reacting with the VP5 antibody (Figure 5C), suggesting possible degradation by exposure to stool proteases.

Mouse pups from vesicle-contained rotavirus- and free rotavirus-inoculated groups were euthanized on days 1 and 3 pi, with total rotavirus levels in their small intestines measured by ELISA (Figure 5D; Table S3) and the number of rotavirus-infected cells visualized by immunofluorescence (Figures 5E and 5F). Significantly higher intestinal levels of rotavirus were measured on day 1 and on day 3 pi in the vesicle-fed compared with free stool rotavirus-fed mouse pups. Note that the intestinal levels of rotavirus detected at 1 dpi of vesicle-fed pups far exceeded the inoculated amounts, a clear indication of viral replication having taken hold. The immunofluorescence staining also revealed significantly higher numbers of infected enterocytes in the vesicle-fed animals compared with free virus-fed ones (Figures 5E and 5F).

Vesicles Remain Intact during Passage through the GI Tract

These results suggested that free independently transmitting rotavirus particles in stools were significantly less infectious, both *in vitro* and *in vivo*, than equal numbers of their vesicle-contained counterparts. One reason for this may be that exposure of their capsids to proteases, antibodies (e.g., secretory IgA) and bile acids within stool and/or the next host's GI tract reduces their infectivity. But another may be that free viruses during fecal-oral transmission become diluted en route in the GI tract of their new host, leading to too few rotaviruses reaching the intestinal enterocytes in numbers sufficient to overcome replication barriers (Chen et al., 2015; Diaz-Munoz et al., 2017). To directly test this idea, we compared the infectivity of vesicle-contained rotaviruses with equivalent and even higher quantities of *vesicle-derived* free rotaviruses (Figure 6).

First, we determined whether vesicles remained intact as they passed through the GI tract, since this would have to be a prerequisite for transporting many rotaviruses together and increasing the MOI at the intestine. Vesicles containing rotavirus were isolated from previously infected mouse pup stools and labeled with CellBrite Fix 488 fluorescent membrane dye. The fluorescent vesicles were then fed into new pups and intestinal contents harvested for visualization after 30 min. Remarkably, the ingested fluorescent vesicles were observed to be intact (Figure 6A), and immunostaining with anti-rotavirus antibodies revealed the viruses to still be retained within them (Figure 6B).

Vesicles Enhance the MOI of Viruses in the GI Tract

Given that the vesicles remained intact as they passed through the GI tract, we next tested whether their potent infection efficiency could be approximated by feeding animals higher quantities of free rotaviruses. Rotavirus-containing vesicles isolated from mouse stools were divided into equal fractions where one fraction was kept intact (1X vesicle virus), one fraction lysed with *non-detergent* hypotonic buffer to free the rotaviruses followed by removal of membranes (1X free virus), one fraction lysed but with freed rotaviruses remaining with the broken vesicle membranes (1X free virus + mem), and a highly concentrated free virus inoculum prepared by pooling multiple lysed vesicle fractions (5X free virus). Mock inoculum consisting of carrier buffers was inoculated into separate animals. Rotavirus quantities of each inoculum was determined by ELISA, and viral loads and volumes normalized before feeding into separate mouse pup groups (Figure 6C; Table S4). Note that none of the buffers used for preparation of the inoculums had any effects on rotavirus infectivity or on the mouse pups (Figure S5; Table S5).

Within 24 hr of feeding the inoculums, both the 1X vesicle virus and the 5X free virus groups began exhibiting severe diarrhea (Figure 6D) and shedding similar quantities of rotavirus into stools (Figure 6E; Table S4). By 3 dpi, the 1X vesicle virus and the 5X free virus groups had similar numbers of rotavirus-infected epithelial cells in their intestines (Figures 6F and 6G). In contrast, the 1X free virus-fed mice began showing diarrhea only at 2 dpi (Figure 6D), shed less rotavirus in their stools, and had far fewer infected intestinal cells (Figures 6E–6G). The 1X free virus + membrane-fed mice had similar levels of infection to 1X free virus, indicating that neither the membranes nor the non-viral vesicle lumen contents were significant modulators of infectivity in these experiments. Collectively these results indicate that the infection efficiency of vesicle-contained rotaviruses can be approximated by feeding animals higher doses of free rotaviruses, and suggest that vesicles are potent vehicles for enteric virus fecal-oral transmission, enabling high multiplicities of infection.

DISCUSSION

Our results here suggest that, during fecal-oral transmission, freely dispersed rotaviruses within stools may not reach intestinal enterocytes in high enough quantities to overcome replication barriers. In contrast, comparable numbers of rotaviruses, by being clustered in populations inside vesicles, can be delivered undiluted to intestinal enterocytes to achieve high multiplicities of infection and overcome these barriers. We had previously observed a similar replication advantage *in vitro* with vesicle-cloaked polioviruses (Chen et al., 2015). The benefits of MOI will likely depend on the virus in question and its target host cells. Viruses that do not carry as many mutations, require fewer

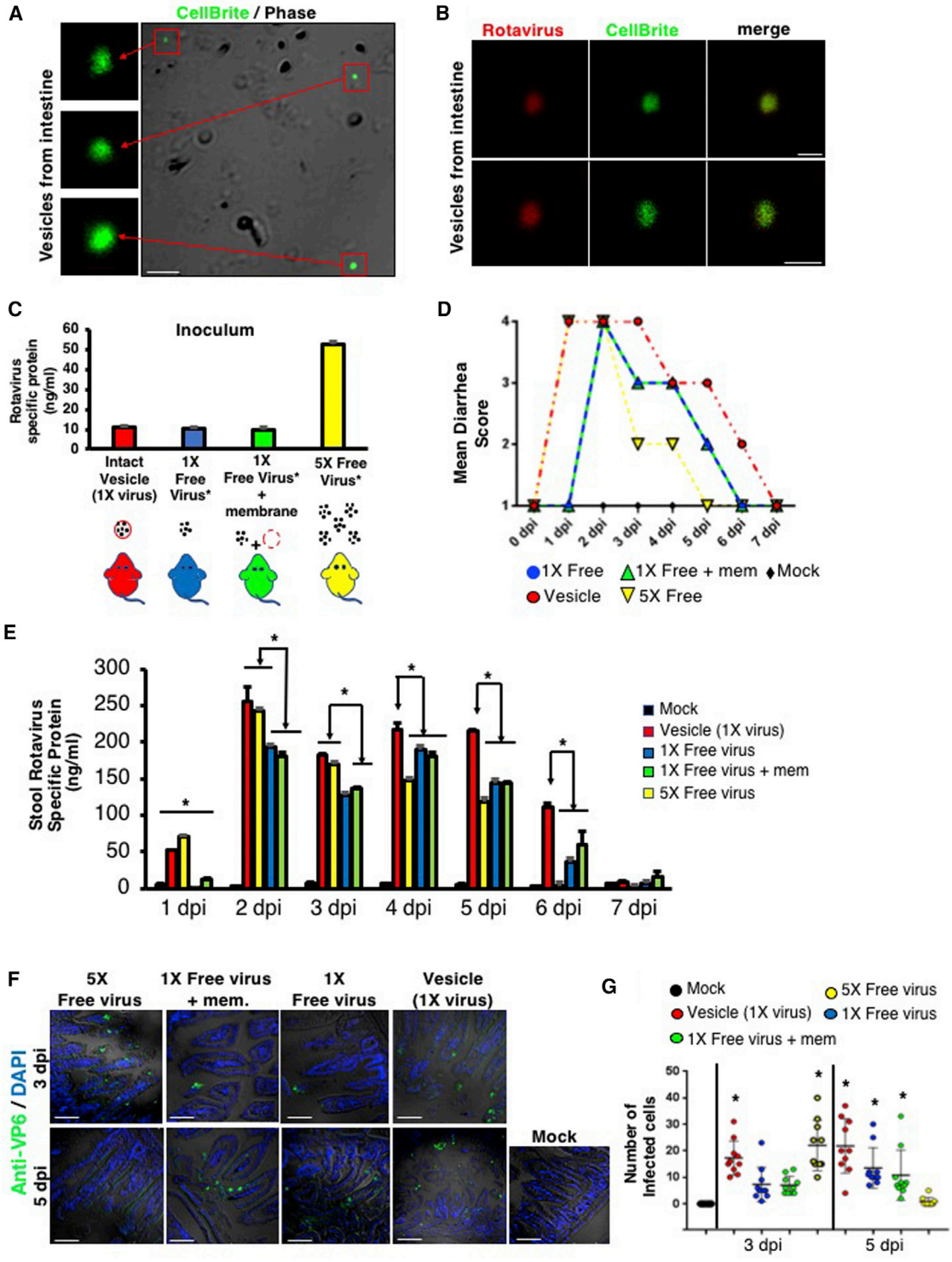

Figure 6. Vesicles Enhance the MOI of Viruses in the Gastrointestinal Tract

(A and B) Vesicles previously isolated from EDIM rotavirus-infected mouse stool samples were stained with CellBrite Fix 488 fluorescent membrane dye and fed to mouse pups. Intestinal contents 30 min post feeding were observed under the confocal microscope live (A) or fixed and immunostained with anti-rotavirus VP6 antibody (B). Representative images from two independent experiments are presented. Scale bars, 2.5 μm (A) and 1 μm (B).

(C) Mouse pups were fed with either mock, intact vesicles (1X virus), 1X free virus, 1X free virus with the vesicle membrane remnants, or 5X free virus. Asterisk (*) denotes that the free virus samples were prepared by lysing the vesicles and releasing their viral contents. Virus inoculum (25 μL) from each group was titrated using ELISA to ensure that equivalent amounts of virus were being fed for each experiment (n = 2). Graph represents the amount of virus that was contained in 25 μL of the inoculum. Each bar in the graph is representative means calculated from the analyses with SD. See Table S4 for raw ELISA data.

(legend continued on next page)

genomes to get replication started, or evade host defenses more efficiently, may not need to be transmitted in as large clusters as rotaviruses or polioviruses. Furthermore the threshold needed may be even lower when infecting cells with weaker innate immune defenses.

The membranes of cargo-transporting EVs including the ones containing rotavirus, norovirus, and poliovirus contain PS lipids with inverted topology. PS lipids are known potent anti-inflammatory molecules (Birge et al., 2016) and also have the ability to bind to and sequester anti-viral cytokines such as interferon gamma (Oyler-Yaniv et al., 2017). Although the membrane remnants co-inoculated with the free rotaviruses did not alter the kinetics of infection (Figure 6, 1X virus ± membrane), it remains to be investigated whether, by being cotransported around the viruses, PS lipids may play a larger role in modulating the immune response. In addition, as we reported here, the vesicle membrane may protect its viral cargo from being degraded through prolonged exposure to stool proteases (Figures 4B and 5C) and recognition by mucosal antibodies within the stool or in the next hosts' gut (Mantis et al., 2011). Indeed invisibility tor antibodies may be one reason why infection appears to be more persistent with vesicle-cloaked viruses (Figures 6D–6G).

Our findings raise intriguing questions regarding rotavirus and norovirus lifecycles. First, how are rotavirus particles able to transfer from the ER lumen to the cytoplasm without ER lysis? Perhaps, as reported with another non-enveloped virus, SV40 (Inoue and Tsai, 2017), chaperones facilitate the transfer of the virus particles across the ER membrane. Secondly, rotaviruses within EVs, isolated from stools or from H69 cell cultures, are already in their activated states with their VP4 cleaved. Where is the cleavage/activation happening? Is it pre- or post-EV packaging? And what is the protease?

We have also found that both human and murine noroviruses appear to exploit the MVB pathway to be released into stool within exosomes. Notably, hepatitis A virus hijacks this pathway to release from liver cells in exosomes (Feng et al., 2013). Whether similar viral cues are utilized by both of these small positive strand RNA viruses to target them to MVBs remains to be investigated. While the receptor for human norovirus is yet to be discovered, we found that the MNV-1 receptor CD300lf was still necessary for infection with MNV-1-containing exosomes and facilitated their internalization into cells. As CD300lf is a well-known member of a large family of PS receptors (Borrego, 2013), it will be important to determine if this protein has a wider role in EV uptake or whether it selectively recognizes MNV-1-containing exosomes, potentially through cues in conjunction with the PS lipids of the vesicles.

In summary, our findings point to vesicle-cloaked viral clusters rather than free viruses as the optimal infectious units in fecal-oral transmission, and demonstrate how vesicles increase the MOI of viruses at target sites by transporting many viral particles together from one host to another. The increased potency of multiple viruses collectively being transmitted raises the possibility that this mode of transmission may be more widely exploited through means other than just vesicles. Indeed, gut bacteria potentially acting as scaffolds to display multiple polioviruses to susceptible cells (Erickson et al., 2018), and enveloped viral particles such as vesicular stomatitis virus and human paramyxoviruses aggregating or inducing cell-to-cell contact, may be strategies to increase MOI during transmission (Cuevas et al., 2017; El Najjar et al., 2016). These findings, together with ours, highlight the need for antiviral therapeutics that disrupt various means of viral clustering including targeting the integrity or production of virus-carrying vesicles, adherence to bacteria, inter-virus tethering, and cell-to-cell contact formation.

STAR★METHODS

Detailed methods are provided in the online version of this paper and include the following:

- KEY RESOURCES TABLE
- CONTACT FOR REAGENT AND RESOURCE SHARING
- EXPERIMENTAL MODEL AND SUBJECT DETAILS
  - Cell Culture
  - Human Enteroid Model
  - Human Stool Samples
  - Mouse Model
  - Piglet Model
  - Virus Propagation
- METHOD DETAILS
  - Fecal and Intestinal Sample Collection
  - Fecal and Intestinal Sample Preparation
  - Vesicle Isolation from Stool, Intestinal Samples and Culture Media
  - Mouse Oral Inoculation
  - Pig Stool Infectivity *In Vitro*
  - Fluorescent Labeling of Isolated Vesicles
  - Immunofluorescence Labeling and Imaging of Cells
  - Immunofluorescence Labeling and Imaging of Tissue Sections
  - Human Norovirus Vesicle/Enteroid Infectivity Assay
  - Real-Time Reverse Transcription-PCR (RT-PCR) Assay
  - CD300fL Antibody Treatment

(D) Stool discharge from animals belonging to all four inoculated groups. A scoring system reported previously (Boshuizen et al., 2003) was utilized where normal dry feces, exceptionally loose feces, loose yellow-green feces, and watery feces corresponded to scores 1, 2, 3, and 4, respectively. Any score above 2 was considered as diarrhea. The diarrheal scores plotted were averaged over two independent experiments.

(E) Stool samples collected each day post-inoculation were analyzed for rotavirus release by ELISA. The results correspond to a mean from two independent experiments with SD (*$p < 0.05$). See Table S4 for raw ELISA data.

(F) Upper small intestinal tissue (duodenum and jejunum) from each inoculated group was processed for immunohistochemistry with antibodies against rotavirus capsids (green) and co-stained with DAPI to visualize the nuclei at 3 and 5 dpi. Representative images from two independent experiments are presented. Scale bars, 100 μm in all panels.

(G) Quantification of the numbers of infected cells within the small intestines from two independent experiments are plotted. Ten independent areas of the small intestines were analyzed for each group. Each individual data point in the graph represents the total number of cells infected in that particular area of interest per group represented along with SD (*$p < 0.05$).

- GW4869 Treatment
- Electron Microscopy
- Immunoprecipitation and Co-immunoprecipitation
- SDS-PAGE and Western Blot Analysis
- MALDI-TOF/MS Lipid Analysis

- QUANTIFICATION AND STATISTICAL ANALYSIS
  - Rotavirus Quantitation by ELISA Assay
  - Diarrhea Scoring of Mouse Feces
  - Statistical Analyses

SUPPLEMENTAL INFORMATION

Supplemental Information includes five figures and five tables and can be found with this article online at https://doi.org/10.1016/j.chom.2018.07.006.

ACKNOWLEDGMENTS

We thank Harry Greenberg (Stanford University); Herbert Virgin (Washington University School of Medicine in St. Louis); Mary Estes (Baylor College of Medicine); Nicholas Mantis (SUNY Albany); Ken Cadwell (New York University); Stephanie Karst (University of Florida); Christiane Wobus (University of Michigan); Erich Mackow (Stony Brook University School of Medicine); Grégoire Altan-Bonnet (National Cancer Institute); Brian Kelsall, Yasmine Belkaid, Nicolas Bouladoux, and Polly Matzinger (National Institute of Allergy and Infectious Diseases); and Altan-Bonnet lab members for reagents, critical discussion, and constructive comments. We also thank James Hawkins, Kristin Demuro, Holly Habbershon, and Amanda Chiedl of the NHLBI animal core and Erin Stempinski of the NHLBI EM core facilities for their technical support in the design and execution of the animal transmission and EM experiments, respectively. P.M.T. and A. Cali were supported by grant R01 AI091985 (NIAID, NIH), and A.N.V and L.J.S were supported by grant R01 A1099451 (NIAID, NIH). A. Cali and P.L. were supported by Sens&Micro LAB Project no. 15 of Regione Puglia and P.L. was also supported by FIR grant no. AYR9D32 of University of Bari. This research was supported in part by the Intramural Research Programs of the NHLBI and NIAID.

AUTHOR CONTRIBUTIONS

Conceptualization and Experiment Design, M.S., S.G., and N.A.-B.; Execution of Experiments, M.S., S.G., B.A.H., V.R., W.-L.D., Y.M., D.A.DeJ.-D., S.V.V., E.A.L., G.I.P., P.M.T., A. Cali, C.B., A.N.V., L.J.S., J.T.P., P.L., A. Corcelli, K.Y.G., and N.A.-B.; Manuscript Writing, M.S., S.G., B.A.H., and N.A.-B.; Supervision, N.A.-B.

DECLARATION OF INTERESTS

The authors declare no competing interests.

Received: November 21, 2017
Revised: June 11, 2018
Accepted: July 13, 2018
Published: August 8, 2018

REFERENCES

Altan-Bonnet, N. (2016). Extracellular vesicles are the Trojan horses of viral infection. Curr. Opin. Microbiol. *32*, 77–81.

Andino, R., and Domingo, E. (2015). Viral quasispecies. Virology *479-480*, 46–51.

Arnold, M., Patton, J.T., and McDonald, S.M. (2009). Culturing, storage, and quantification of rotaviruses. Curr. Protoc. Microbiol. *Chapter 15*, 15C.3.1-15C.3.24.

Arnold, M.M., Brownback, C.S., Taraporewala, Z.F., and Patton, J.T. (2012). Rotavirus variant replicates efficiently although encoding an aberrant NSP3 that fails to induce nuclear localization of poly(A) binding protein. J. Gen. Virol. *93*, 1483–1494.

Bird, S.W., Maynard, N.D., Covert, M.W., and Kirkegaard, K. (2014). Nonlytic viral spread enhanced by autophagy components. Proc. Natl. Acad. Sci. USA *111*, 13081–13086.

Birge, R.B., Boeltz, S., Kumar, S., Carlson, J., Wanderley, J., Calianese, D., Barcinski, M., Brekken, R.A., Huang, X., Hutchins, J.T., et al. (2016). Phosphatidylserine is a global immunosuppressive signal in efferocytosis, infectious disease, and cancer. Cell Death Differ. *23*, 962–978.

Bok, K., Abente, E.J., Realpe-Quintero, M., Mitra, T., Sosnovtsev, S.V., Kapikian, A.Z., and Green, K.Y. (2009). Evolutionary dynamics of GII.4 noroviruses over a 34-year period. J. Virol. *83*, 11890–11901.

Bordería, A.V., Isakov, O., Moratorio, G., Henningsson, R., Agüera-González, S., Organtini, L., Gnädig, N.F., Blanc, H., Alcover, A., Hafenstein, S., et al. (2015). Group selection and contribution of minority variants during virus adaptation determines virus fitness and phenotype. PLoS Pathog. *11*, e1004838.

Borrego, F. (2013). The CD300 molecules: an emerging family of regulators of the immune system. Blood *121*, 1951–1960.

Boshuizen, J.A., Reimerink, J.H., Korteland-van Male, A.M., van Ham, V.J., Koopmans, M.P., Büller, H.A., Dekker, J., and Einerhand, A.W. (2003). Changes in small intestinal homeostasis, morphology, and gene expression during rotavirus infection of infant mice. J. Virol. *77*, 13005–13016.

Burns, J.W., Krishnaney, A.A., Vo, P.T., Rouse, R.V., Anderson, L.J., and Greenberg, H.B. (1995). Analyses of homologous rotavirus infection in the mouse model. Virology *207*, 143–153.

Chen, Y.H., Du, W., Hagemeijer, M.C., Takvorian, P.M., Pau, C., Cali, A., Brantner, C.A., Stempinski, E.S., Connelly, P.S., Ma, H.C., et al. (2015). Phosphatidylserine vesicles enable efficient en bloc transmission of enteroviruses. Cell *160*, 619–630.

Coots, A., Donnelly, B., Mohanty, S.K., McNeal, M., Sestak, K., and Tiao, G. (2012). Rotavirus infection of human cholangiocytes parallels the murine model of biliary atresia. J. Surg. Res. *177*, 275–281.

Crawford, S.E., Mukherjee, S.K., Estes, M.K., Lawton, J.A., Shaw, A.L., Ramig, R.F., and Prasad, B.V. (2001). Trypsin cleavage stabilizes the rotavirus VP4 spike. J. Virol. *75*, 6052–6061.

Cuevas, J.M., Duran-Moreno, M., and Sanjuan, R. (2017). Multi-virion infectious units arise from free viral particles in an enveloped virus. Nat. Microbiol. *2*, 17078.

Diaz-Munoz, S.L., Sanjuan, R., and West, S. (2017). Sociovirology: conflict, cooperation and communication among viruses. Cell Host Microbe *22*, 437.

El Najjar, F., Cifuentes-Muñoz, N., Chen, J., Zhu, H., Buchholz, U.J., Moncman, C.L., and Dutch, R.E. (2016). Human metapneumovirus induces reorganization of the actin cytoskeleton for direct cell-to-cell spread. PLoS Pathog. *12*, e1005922.

Erickson, A.K., Jesudhasan, P.R., Mayer, M.J., Narbad, A., Winter, S.E., and Pfeiffer, J.K. (2018). Bacteria facilitate enteric virus co-infection of mammalian cells and promote genetic recombination. Cell Host Microbe *23*, 77.

Ettayebi, K., Crawford, S.E., Murakami, K., Broughman, J.R., Karandikar, U., Tenge, V.R., Neill, F.H., Blutt, S.E., Zeng, X.L., Qu, L., et al. (2016). Replication of human noroviruses in stem cell-derived human enteroids. Science *353*, 1387–1393.

Feng, Z., Hensley, L., McKnight, K.L., Hu, F., Madden, V., Ping, L., Jeong, S.H., Walker, C., Lanford, R.E., and Lemon, S.M. (2013). A pathogenic picornavirus acquires an envelope by hijacking cellular membranes. Nature *496*, 367–371.

Gould, S.J., and Raposo, G. (2013). As we wait: coping with an imperfect nomenclature for extracellular vesicles. J. Extracell. Vesicles *2*, https://doi.org/10.3402/jev.v2i0.2038.

Greenberg, H.B., and Estes, M.K. (2009). Rotaviruses: from pathogenesis to vaccination. Gastroenterology *136*, 1939–1951.

Grubman, S.A., Perrone, R.D., Lee, D.W., Murray, S.L., Rogers, L.C., Wolkoff, L.I., Mulberg, A.E., Cherington, V., and Jefferson, D.M. (1994). Regulation of intracellular pH by immortalized human intrahepatic biliary epithelial cell lines. Am. J. Physiol. *266*, G1060–G1070.

Haraszti, R.A., Didiot, M.C., Sapp, E., Leszyk, J., Shaffer, S.A., Rockwell, H.E., Gao, F., Narain, N.R., DiFiglia, M., Kiebish, M.A., et al. (2016). High-resolution

proteomic and lipidomic analysis of exosomes and microvesicles from different cell sources. J. Extracell Vesicles *5*, 32570.

Inoue, T., and Tsai, B. (2017). Regulated Erlin-dependent release of the B12 transmembrane J-protein promotes ER membrane penetration of a non-enveloped virus. PLoS Pathog. *13*, e1006439.

Kapikian, A.Z., Wyatt, R.G., Dolin, R., Thornhill, T.S., Kalica, A.R., and Chanock, R.M. (1972). Visualization by immune electron microscopy of a 27-nm particle associated with acute infectious nonbacterial gastroenteritis. J. Virol. *10*, 1075–1081.

Karst, S.M., Wobus, C.E., Goodfellow, I.G., Green, K.Y., and Virgin, H.W. (2014). Advances in norovirus biology. Cell Host Microbe *15*, 668–680.

Kowal, J., Tkach, M., and Thery, C. (2014). Biogenesis and secretion of exosomes. Curr. Opin. Cell Biol. *29*, 116–125.

Levenson, E.A., Martens, C., Kanakabandi, K., Turner, C., Virtaneva, K., Paneru, M., Ricklefs, S., Sosnovtsev, S.V., Johnson, J.A., Porcella, S.F., et al. (2018). Comparative transcriptomic response of primary and immortalized macrophages to murine norovirus infection. J. Immunol. *200*, 4157–4169.

Mantis, N.J., Rol, N., and Corthesy, B. (2011). Secretory IgA's complex roles in immunity and mucosal homeostasis in the gut. Mucosal Immunol. *4*, 603–611.

McConnell, R.E., Higginbotham, J.N., Shifrin, D.A., Jr., Tabb, D.L., Coffey, R.J., and Tyska, M.J. (2009). The enterocyte microvillus is a vesicle-generating organelle. J. Cell Biol. *185*, 1285–1298.

Miyanishi, M., Tada, K., Koike, M., Uchiyama, Y., Kitamura, T., and Nagata, S. (2007). Identification of Tim4 as a phosphatidylserine receptor. Nature *450*, 435–439.

Mohl, B.P., and Roy, P. (2014). Bluetongue virus capsid assembly and maturation. Viruses *6*, 3250.

Nair, N., Feng, N., Blum, L.K., Sanyal, M., Ding, S., Jiang, B., Sen, A., Morton, J.M., He, X.S., Robinson, W.H., and Greenberg, H.B. (2017). VP4- and VP7-specific antibodies mediate heterotypic immunity to rotavirus in humans. Sci. Transl. Med. *9*, https://doi.org/10.1126/scitranslmed.aam5434.

Orchard, R.C., Wilen, C.B., Doench, J.G., Baldridge, M.T., McCune, B.T., Lee, Y.C., Lee, S., Pruett-Miller, S.M., Nelson, C.A., Fremont, D.H., et al. (2016). Discovery of a proteinaceous cellular receptor for a norovirus. Science *353*, 933–936.

Oyler-Yaniv, J., Oyler-Yaniv, A., Shakiba, M., Min, N.K., Chen, Y.H., Cheng, S.Y., Krichevsky, O., Altan-Bonnet, N., and Altan-Bonnet, G. (2017). Catch and release of cytokines mediated by tumor phosphatidylserine converts transient exposure into long-lived inflammation. Mol. Cell *66*, 635–647.e7.

Parra, G.I., Azure, J., Fischer, R., Bok, K., Sandoval-Jaime, C., Sosnovtsev, S.V., Sander, P., and Green, K.Y. (2013). Identification of a broadly cross-reactive epitope in the inner shell of the norovirus capsid. PLoS One *8*, e67592.

Ramani, S., Atmar, R.L., and Estes, M.K. (2014). Epidemiology of human noroviruses and updates on vaccine development. Curr. Opin. Gastroenterol. *30*, 25–33.

Robinson, S.M., Tsueng, G., Sin, J., Mangale, V., Rahawi, S., McIntyre, L.L., Williams, W., Kha, N., Cruz, C., Hancock, B.M., et al. (2014). Coxsackievirus B exits the host cell in shed microvesicles displaying autophagosomal markers. PloS Pathog. *10*, e1004045.

Saxena, K., Blutt, S.E., Ettayebi, K., Zeng, X.L., Broughman, J.R., Crawford, S.E., Karandikar, U.C., Sastri, N.P., Conner, M.E., Opekun, A.R., et al. (2015). Human intestinal enteroids: a new model to study human rotavirus infection, host restriction, and pathophysiology. J. Virol. *90*, 43–56.

Shao, L., Fischer, D.D., Kandasamy, S., Rauf, A., Langel, S.N., Wentworth, D.E., Stucker, K.M., Halpin, R.A., Lam, H.C., Marthaler, D., et al. (2015). Comparative in vitro and in vivo studies of porcine rotavirus G9P[13] and human rotavirus Wa G1P[8]. J. Virol. *90*, 142–151.

Skotland, T., Sandvig, K., and Llorente, A. (2017). Lipids in exosomes: current knowledge and the way forward. Prog. Lipid Res. *66*, 30–41.

Small, C., Barro, M., Brown, T.L., and Patton, J.T. (2007). Genome heterogeneity of SA11 rotavirus due to reassortment with "O" agent. Virology *359*, 415–424.

Sosnovtsev, S.V., Belliot, G., Chang, K.O., Prikhodko, V.G., Thackray, L.B., Wobus, C.E., Karst, S.M., Virgin, H.W., and Green, K.Y. (2006). Cleavage map and proteolytic processing of the murine norovirus nonstructural polyprotein in infected cells. J. Virol. *80*, 7816–7831.

Trask, S.D., McDonald, S.M., and Patton, J.T. (2012). Structural insights into the coupling of virion assembly and rotavirus replication. Nat. Rev. Microbiol. *10*, 165–177.

Urbanelli, L., Magini, A., Buratta, S., Brozzi, A., Sagini, K., Polchi, A., Tancini, B., and Emiliani, C. (2013). Signaling pathways in exosomes biogenesis, secretion and fate. Genes (Basel) *4*, 152–170.

van Niel, G., D'Angelo, G., and Raposo, G. (2018). Shedding light on the cell biology of extracellular vesicles. Nat. Rev. Mol. Cell Biol. *19*, 213–228.

Wobus, C.E., Thackray, L.B., and Virgin, H.W., 4th (2006). Murine norovirus: a model system to study norovirus biology and pathogenesis. J. Virol. *80*, 5104–5112.

Yin, X., Ambardekar, C., Lu, Y., and Feng, Z. (2016). Distinct entry mechanisms for nonenveloped and quasi-enveloped hepatitis E viruses. J. Virol. *90*, 4232–4242.

STAR★METHODS

KEY RESOURCES TABLE

REAGENT or RESOURCE	SOURCE	IDENTIFIER
Antibodies		
Sheep polyclonal anti-Rotavirus	GeneTex	Cat#GTX39230; RRID: AB_11166691
Mouse monoclonal anti-RVVP5	Nair et al., 2017	N/A
Guinea pig polyclonal anti-RVVP6	Arnold et al., 2012	N/A
Guinea pig polyclonal anti-RVVP7	Nair et al., 2017	N/A
Goat anti-mouse CD300f/LMIR3	R&D Systems	Cat#AF2788; RRID: AB_2244388
Mouse monoclonal anti-NVVP1	Parra et al., 2013	N/A
Guinea pig polyclonal anti-MNVVP1	Sosnovtsev et al., 2006	N/A
Rabbit polyclonal anti-LC3A/B	Cell Signaling	Cat#4108S; RRID: AB_2137703
Rabbit polyclonal anti-Sec61β	Affinity BioReagents	Cat#PA3-015; RRID: AB_2239072
Rabbit polyclonal anti-CD98	GeneTex	Cat#GTX54716;
Mouse monoclonal anti-GAPDH	Santa Cruz	Cat#SC-47724; RRID: AB_627678
Mouse monoclonal anti-Actin	Abcam	Cat#ab3280; RRID: AB_303668
Bacterial and Virus Strains		
Simian Rotavirus SA114F strain	Small et al., 2007	N/A
Murine Rotavirus EDIM strain	Burns et al., 1995	N/A
Murine Norovirus MNV-1 strain	Sosnovtsev et al., 2006	N/A
Human Rotavirus WA G1P[8] strain	Shao et al., 2015	N/A
Human Norovirus HuNoV/GII.4 strain isolated from patients	NIH Clinical Center	N/A
Biological Samples		
Human derived fecal samples isolated from patients	NIH Clinical Center	N/A
Piglet derived fecal samples	Shao et al., 2015	N/A
Piglet derived large intestinal content samples	Shao et al., 2015	N/A
Mouse derived gastrointestinal samples	This paper	N/A
Mouse derived fecal samples	This paper	N/A
Chemicals, Peptides, and Recombinant Proteins		
GW4869 (hydrochloride hydrate)	Cayman Chemical	Cat#13127; CAS: 6823-69-4
CellBrite Fix 488	Biotium	30090-T
BEGM SingleQuot Kit	Lonza	CC-4175
Critical Commercial Assays		
Fecal Rotavirus Antigen ELISA Kit	Epitope Diagnostics	KTR 841
MagCapture Exosome Isolation Kit PS	FUJIFILM Wako Pure Chemical	293-77601
Annexin V MicroBead Kit	MACS Miltenyi Biotec	130-090-201
ExoCap Composite Kit for Serum Plasma	JSR Life Sciences	EX-COM-SP
Detergent-Free Exosomal Protein Extraction Kit	101Bio	P201
MagMax-96 Viral Isolation Kit	Shao et al., 2015	N/A
QuantiTect SYBR green RT-PCR Kit	Shao et al., 2015	N/A
Experimental Models: Cell Lines		
Monkey kidney cells (MA104)	Arnold et al., 2009	ATCC CRL-2378.1, RRID: CVCL_3846
Human biliary epithelial cells (H69)	Grubman et al., 1994	N/A
Human colon adenocarcinoma cells (CACO2)	ATCC	ATCC HTB-37, RRID: CVCL_0025
Jejunal-derived human intestinal enteroids (J2, Sec+)	Saxena et al., 2015	N/A
Murine macrophage-like cells (RAW264.7)	Sosnovtsev et al., 2006	ATCC TIB-71, RRID: CVCL_0493

(*Continued on next page*)

Continued

REAGENT or RESOURCE	SOURCE	IDENTIFIER
Experimental Models: Organisms/Strains		
Mouse: BALB/cJ	The Jackson Laboratory	000651
Pig: Gnotbiotic and Wild type piglets born to landrance-yorkshire breed sows	Shao et al., 2015	N/A
Oligonucleotides		
6FAM GII-Probe TGGGAGGGCGATC	Bok et al., 2009	N/A
GII-Forward ATGTTYAGRTGGATGAGRTT	Bok et al., 2009	N/A
GII-Reverse ACGCCATCTTCATTCACA	Bok et al., 2009	N/A
ORF1 specific forward primer GGCTACGGCTGGACATGTCT	Levenson et al., 2018	N/A
ORF1 specific reverse primer GCGTCAGGCCTATCCTCCTT	Levenson et al., 2018	N/A
6FAM-BHQ1 labeled probe CTATCTTCCGCCGTTACCCCC ATCTG	LGC Biosearch Technologies	N/A
ORF1 PCR amplicon TCTGATCCGTGGCTACGGCTGGACATG TCTGATAAGGCTATCTTCCGCCGTTACCCCCATCTGCGGCCT AAGGAGGATAGGCCTGACGCGCCCTCCCATG	LGC Biosearch Technologies	N/A
Software and Algorithms		
Synergy H1 Multi-Mode Reader Gen5 Software	BioTek	N/A
GraphPad Prism 7.02 Software	GraphPad Prism	N/A
ZEN 2.3 SP1 Black	Carl Zeiss	N/A
ImageQuant TL 8.1	Amersham	29-0007-37
Other		
Bovine Serum Albumin (BSA)	Fisher Scientific	BP1600-100
Paraformaldehyde (PFA) 16% Solution	Electron Microscopy Sciences	15710
Phosphate-Buffered Saline (PBS)	Fisher Scientific	BP399-20
Dulbecco's Phosphate-Buffered Saline (DPBS)	Gibco	14190-144
Saponin from quillaja bark (SAP)	Sigma-Aldrich	S4521
Formaldehyde (FA)	EMD	FX0410-5
Gluteraldehyde 8% Solution (Glut)	Electron Microscopy Sciences	16019
Fluormount G with DAPI	Electron Microscopy Sciences	17984-24
Dulbecco's Modification of Eagle's Medium (DMEM)	Corning Cellgro	10-013-CV
Medium 199 (M199)	Corning Cellgro	10-060-CV
Penicillin-Streptomycin (P/S) solution	Corning	30-002-CI
Fetal Bovine Serum Heat-Inactivated (FBS-HI)	Atlas Biologicals	EF-0050-A
TWEEN-20	Sigma Aldrich	P2287
Tris Buffered Saline (TBS)	Bio-Rad	170-6435
Tris-Glycine-SDS Buffer	Bio-Rad	161-0732
Blotting-Grade Blocker	Bio-Rad	170-6404
Sodium Azide (NaN_3)	Fisher Scientific	S227I-25
4x Laemli Sample Buffer	Bio-Rad	161-0747
Protein Assay Dye	Bio-Rad	5000006
Trichloroacetic Acid (TCA)	Fisher Scientific	A-322-100
Eagle's Minimal Essential Media (EMEM)	Lonza	12-125F
Beta Mercaptoethanol (BME)	Sigma	M7154
Protean TGX pre-cast gels	Bio-Rad	456-1034
Cell Lysis Buffer	BD Pharmingen	51-6636KC
Trans-Blot Turbo transfer pack	Bio-Rad	170-4159
Halt Phosphatase inhibitor	Thermo Fisher	1862495

(*Continued on next page*)

Continued

REAGENT or RESOURCE	SOURCE	IDENTIFIER
Halt Protease inhibitor	Thermo Fisher	1861278
Plastic feeding tubes	Instech Lab	FTP-22-25
Polycarbonate ultracentrifuge tubes	Beckman	Cat#355631; 355630; 343776
Poly-L-Lysine	Sigma Aldrich	P4707

CONTACT FOR REAGENT AND RESOURCE SHARING

Further information and requests for resources and reagents should be directed to and will be fulfilled by the Lead Contact, Nihal Altan-Bonnet (nihal.altan-bonnet@nih.gov).

EXPERIMENTAL MODEL AND SUBJECT DETAILS

Cell Culture

MA104 Cells

MA-104 Clone 1 was purchased from the American Type Culture Collection (ATCC CRL-2378., RRID: CVCL_3846). These are embryonic kidney epithelial cells from *Cercopethecus aethiops* of unspecified sex. Cells were maintained in M199 media supplemented with 1% Pen/Strep, 10% FBS-HI and incubated at 37°C/5%CO_2.

H69 Cells

H69 cells (RRID: CVCL_8121) are immortalized human intrahepatic biliary epithelial cells. They were isolated from human brain dead organ donors of unspecified age and sex under protocol approved by the Institutional Review Board of the New England Medical Center (Grubman et al., 1994). Cells were maintained in DMEM supplemented with BEGM SingleQuot Kit and 5% FBS-HI and incubated at 37°C/5%CO_2.

RAW264.7

RAW264.7 cells were purchased from ATCC (ATCC TIB-71, RRID: CVCL_0493). These are macrophages isolated from adult male BALB/c mice. Cells were maintained in DMEM supplemented with 1% Pen/Strep, 10% FBS-HI and incubated at 37°C/5%CO_2.

CACO-2

CACO-2 cells were purchased from the ATCC (ATCC HTB-37, RRID: CVCL_0025). These are epithelial cells isolated from a 72 year old male human. Cells were maintained in EMEM media supplemented with 1% Pen/Strep, 20% FBS-HI and incubated at 37°C/5%CO_2.

Human Enteroid Model

Human enteroid samples were a kind gift of Dr. Mary Estes (Baylor College of Medicine, Dallas, TX). Briefly, jejunal tissue was obtained from adult patients undergoing bariatric surgery (Baylor College of Medicine Institutional Review Board approved study protocols H-13793 and H-31910). Enteroids were maintained as described previously by Saxena et al. (2015).

Human Stool Samples

Stool specimens (positive or negative for norovirus) were from pediatric patients (6 years of age or younger, three male and one female) enrolled in protocols approved by the institutional review board of the National Institute of Allergy and Infectious Diseases, with informed parental consent.

Mouse Model

BALB/cJ mice were purchased from The Jackson Laboratory (Stock: 000651) and all animals were housed and bred in-house (animals that aged more than 5–6 weeks) in accordance with the procedure outlined in the Guide for the Care and Use of Laboratory Animals under an animal study proposal approved by the NHLBI Animal Care and Use Committee. Briefly, the animal facility temperature was maintained at 72°F, the animals were housed in ventilated racks and the cages were supplied with hardwood bedding and Nest packs. Animals were provided the NIH 31 feed and autoclaved water. A 6am-6pm light cycle was followed. All animal experiments were performed in an American Association for the Accreditation of Laboratory Animal Care (AAALAC) accredited animal facility. For the purpose of experiments all pups that were used for the study were of 10 days old. We did not gender the pups in the litters but it was always a mix of females and males and gendering was not deemed necessary as rotavirus infections do not show any gender bias. Animal euthanization was also done as per the AAALAC guidelines where adult animals were euthanized by CO_2 exposure (USP Grade A) at 3 litres/min. Approximately it took 2-3 minutes to anaesthetize the animals with a 10-30% filled up CO_2 chamber when lack of respiration and faded eye color was observed. CO_2 flow was maintained for a minimum of 1 minute after respiration ceased.

Piglet Model

Gnotobiotic (Gn) piglets were derived and maintained as previously described (Shao et al., 2015). Near-term sows (Landrace × Yorkshire × Duroc cross-bred) were purchased from the Ohio State University Swine Center facility. Caesarean-derived piglets transplanted with complete human microbiota were housed individually in positive-pressure sterile isolators (to ensure no environmental contamination), in temperature-controlled rooms with a 12 h light/dark cycles. All piglets were confirmed negative for rotavirus, astrovirus, and kobuvirus. The piglets were fed 2 times a day with ultra-high temperature pasteurized (UHT) bovine milk (Parmalat) that met or exceeded the National Research Council (NRC) Animal Care Committee's guidelines for calories, fat, protein and carbohydrates in suckling piglets. Piglets were inoculated at 24 days old with HRV Wa. Fecal samples and intestinal contents were collected on day 2 post-HRV inoculation. Piglets were not gendered in these litters, but it was always a mix of females and males. All piglets were humanely euthanized by electrocution following anesthesia.

Virus Propagation

Simian Rotavirus

SA114F (sRV) strain was propagated in MA104 cells according to protocol from Arnold et al. (2009); in brief, $2x10^6$ cells were seeded in 150mm cell culture dishes and incubated for 48hr. Media was removed and replaced with serum free media (SFM). Cells were infected with activated rotavirus (with 10μg/ml of porcine trypsin at 37°C) and was added to cell cultures at an MOI of 0.1 and incubated for 1hr at 37°C/5%CO_2. Finally, cells were rinsed and further incubated with pre warmed SFM until CPE was visible. Cell cultures were freeze-thawed 3 times, media was collected and cell debris removed by centrifugation (1000x g for 15 minutes). Cleared stock virus was aliquoted and stored at -80°C until ready to use.

Murine Rotavirus

EDIM (Epizootic Diarrhea of Infant Mice) strain was kindly provided by Dr. H. Greenberg (Stanford University, Palo Alto, CA) and was propagated in BALB/cJ mice. Five-day old mouse pups were orally infected with 100 fold diluted stock virus in 1X PBS and 2 dpi (day post infection), when the animals started to have diarrhea they were euthanized by decapitation. Intestines were surgically extracted and the tissues were homogenized in M199 medium and centrifuged at 5000 rpm for 10 minutes at 4°C to isolate the virus from the tissue. The stock virus was aliquoted and stored at -80°C.

Murine Norovirus

MNV-1 (mNV) strain was propagated in RAW264.7 cells according to protocol in Sosnovtsev et al. (2006). In brief, $1x10^7$ cells were seeded in 150mm cell culture dishes and incubated for 48hr. Cells were infected with mNV at an MOI of 0.1 and incubated for 1hr at 37°C/5%CO_2. Finally, cells were rinsed and further incubated with pre-warmed SFM until CPE was visible. Cell cultures were freeze-thawed 3 times, media was collected and cell debris removed by centrifugation (1000x g for 15 minutes). Cleared stock virus was aliquoted and stored at -80°C until ready to use.

METHOD DETAILS

Fecal and Intestinal Sample Collection

Human Rotavirus

WA G1P[8] strain infected large intestinal samples from gnotobiotic (Gn) piglets or feces were collected at 2 days post infection. Infection and collection was performed previously described in Shao et al. (2015). In brief, one week old Gn and WT piglets received 5ml of 100mM $NaHCO_3$ to reduce gastric acidity immediately before inoculation; then rotavirus was given orally using a needless syringe at a dose of 10^5 fluorescence-forming units (3-5ml).

Murine Rotavirus

EDIM infected mouse fecal samples were collected at 2-5 days post infection from 5-day old mouse pups that were orally infected with 100 fold diluted stock virus diluted 1X PBS.

Fecal and Intestinal Sample Preparation

Clarified Stool and Intestinal Solutions

All fecal and intestinal content samples were prepared as 5 or 10% solution in 1xDPBS and subjected to a series of sequential centrifugation steps from 500x g to 5,000x g (transferring the supernatants to a new tube at every 1000x g increments) at 10°C to remove debris.

Vesicle Depleted Stool Solutions

Clarified stools were subjected to an additional centrifugation step at 10,000x g for 30 minutes plus 2 consecutive rounds of vesicle isolation procedure described in the Vesicle Isolation section.

Low centrifugation speeds were carried out on a bench top refrigerated centrifuge from Eppendorf; and high centrifugation speeds were carried out on the Beckman L8-80M or TL-100 Ultracentrifuges.

Vesicle Isolation from Stool, Intestinal Samples and Culture Media

All vesicles either from cell culture or clarified intestinal contents and fecal solutions were isolated using one of the following kits according to manufacturer's specifications: Annexin V MicroBead Kit uses Annexin V coated magnetic beads. MagCapture Exosome Isolation Kit PS uses TIM4 coated magnetic beads. ExoCap Composite Kit uses a mixture of CD9, CD63, CD81, and EpCAM coated

magnetic beads. In summary, all cleared samples (as specified below) were incubated with the selected magnetic beads to allow vesicles to bind to the beads. The bead-vesicle complexes were then separated from the sample, using a magnetic strip for 1 minute at RT, and washed 3 times with the buffer included in the kit; finally, the bead bound vesicles were eluted from the beads for further processing.

Cell Culture Vesicles

Confluent cell monolayers in 150mm cell culture dishes were infected with stock virus (MOI 1) and incubated for 1hr at 37°C/5%CO_2, then the inoculum was removed by rinsing the cells with pre-warmed SFM and further incubated in 20ml of SFM. Culture media collected from infected cell cultures (sRV 12 hpi, mNV 24 hpi) were subjected to 3 sequential centrifugation steps at 10°C: at 500x g for 20 minutes to remove cell debris, then the cleared media was transferred to polycarbonate ultracentrifuge tubes and centrifuged at 10000x g for 30 minutes, pellet was collected and supernatant was centrifuged at 100000x g for 1hr to collect the different fraction pellets containing extracellular vesicles. Finally, pellets were resuspended in 1ml of SFM and stored at 4°C until ready for the pull down.

Fecal and Intestinal Content Vesicles

1ml of 5% or 10% clarified stool or gut content solutions (see stool solutions) were used to isolate vesicles.

Mouse Oral Inoculation

Isolated Vesicle or Free Virus Inoculation

Ten day old mouse pups, kept in 5 different cages, were inoculated by oral gavage with one of these four: intact vesicle, free virus, free virus + membrane, 5X free virus, or mock (fed with vehicle buffer). Stool samples were collected each day until day 7 post infection. A subset of animals was sacrificed at 3 and 5 days post infection (dpi) to harvest the small intestine. The small intestines (upper part consisting of duodenum and jejunum) were excised, swiss-rolled, and fixed overnight in 4% PFA. Isolated fecal vesicles were divided into 4 fractions in a ratio 1:1:1:5. One intact fraction (1X) was kept aside for feeding mouse pups as ''Intact Vesicles''. The other fractions were lysed using Detergent-free Exosomal Protein Extraction Kit, as per the manufacturer's protocol, to release the virus particles from the vesicles. One lysed fraction was left with the vesicle membranes along with the free viruses for feeding the mouse pups as ''Free Virus + Membrane''. From the other two lysed fractions (1X and 5X) the left over membranes were removed by centrifugation and were used for feeding the mouse pups as ''Free Virus'' and ''5X Free Virus'', respectively. Inoculum amounts of virus were verified by ELISA assay with the EDI Fecal Rotavirus Antigen ELISA Kit using 25μl of sample from each group.

Vesicle Depleted Stool Inoculation

For this experiment, 2 cages of mouse pups (10 day old; n = 4 animals per cage) were inoculated with vesicle depleted stool or intact vesicles containing, both containing equivalent amounts of EDIM particles. Mice were monitored for diarrhea and stools collected. A subset of animals was sacrificed at 1 and 3 dpi and their small intestines collected to analyze the viral load by ELISA (EDI Fecal Rotavirus Antigen ELISA Kit) or immunohistochemistry.

Pig Stool Infectivity *In Vitro*

MA104 cells seeded to confluency in multi-well plates were inoculated with an aliquot of 5% or 10% clarified fecal solution (complete or vesicle depleted) and incubated for 1hr at 37°C/5% CO_2. Then inoculum was removed by rinsing cells with pre-warmed serum free media and further incubated for the required time. Finally, cells were rinsed with 1xPBS and lysed using cell lysis buffer supplemented with protease and phosphatase inhibitors. Lysates were centrifuged and supernatants were stored at -20°C until further processing.

Fluorescent Labeling of Isolated Vesicles

Vesicles were labeled using CellBrite Fix 488 according to manufacturer protocol. In brief, TIM4 isolated vesicles for mouse feeding were labeled in solution by resuspending them in 500μl of elution buffer containing CellBrite and incubated at 37°C for 15 minutes. Labeled vesicles were washed 3 times with elution buffer followed by centrifugation at 10000x g for 15 minutes. Isolated vesicles for imaging were added to Poly-L-Lysine coated coverslips and allowed to attach for 30 minutes at RT; followed by CellBrite incubation in 1xPBS at 37°C for 15 minutes; they were then fixed in 4% paraformaldehyde in 1xPBS; and finally immunolabeled (as described below) with the anti-Rotavirus antibody, and mounted on glass slides for imaging. Imaging was performed on a Zeiss LSM780 Confocal Laser Scanning or the Zeiss ELYRA PS.1 Super Resolution microscope.

Immunofluorescence Labeling and Imaging of Cells

Cells were seeded on glass cover slips and incubated for 24 hours at 37°C/5%CO_2; then cells were infected with virus stock and fixed at different time points (as needed for each experiment) in 4% PFA in 1xPBS for 10 minutes at room temperature (RT) followed by 3 washes with 1xPBS. Fixed samples were incubated with primary antibodies diluted in incubation buffer (1xPBS supplemented with 1% BSA and 0.2% SAP) for 1hr at RT and washed 3 times 5 minutes each with 1xPBS; then samples were incubated in fluorescently tagged secondary antibodies (either anti-mouse, anti-sheep, anti-guinea pig, or anti-rabbit) diluted in incubation buffer for 1hr at RT in the dark and washed 3 times with 1xPBS. Finally, samples were mounted with Fluoromount G on glass slides and imaged. Imaging was performed on a Zeiss LSM780 Confocal Laser Scanning or the Zeiss ELYRA PS.1 Super Resolution microscope.

Immunofluorescence Labeling and Imaging of Tissue Sections

Small intestine samples were collected from euthanized mice, as each experiment required, and made into Swiss Rolls. Samples were then fixed overnight at 4°C in 4% PFA. Later, samples were incubated for 24hr in 30% sucrose solution at 4°C, and embedded in O.C.T. compound before frozen sectioning on a microtome, Leica Cryo-start CM3050S.

Immunofluorescence Labeling

Frozen tissue sections were permeabilized for 2hr at RT with 0.1% Triton X100 in 1xDPBS supplemented with 10% FBS. Then, samples were incubated overnight at 4°C in primary antibody diluted in 1xDPBS supplemented with 10% FBS. Next, samples were rinsed 3 times with 1xDPBS and incubated for 2hr at RT in fluorescently labeled secondary antibodies diluted in 1xDPBS supplemented with 10% FBS. Finally, samples were rinsed 3 times with 1xDPBS and mounted using Fluormount G containing DAPI stain. Imaging was performed on a Zeiss LSM780 Confocal Laser Scanning microscope.

Human Norovirus Vesicle/Enteroid Infectivity Assay

Monolayers of differentiated jejunal-derived human intestinal enteroids (J2, Sec+) were inoculated with a 2.5X dilution of the TIM-4 isolated vesicles, which represented an average of $\sim 3.5 \times 10^5$ norovirus genome equivalents per well. Monolayers were carefully washed 3 times after incubating for 1hr to allow for absorption and further incubated for 93hrs at 37°C. Norovirus RNA was extracted using the MagMax-96 Viral Isolation kit following manufacturer's protocol. Viral detection was performed by RT-qPCR. Experiment was performed in triplicate.

Real-Time Reverse Transcription-PCR (RT-PCR) Assay

Human Norovirus

Human norovirus genome copies was determined using the oligos GII-Probe (6FAM- TGG GAG GGC GAT C), GII-Forward (ATGTTYAGRTGGATGAGRTT) and GII-Reverse (ACGCCATCTTCATTCACA) as previously described (Bok et al., 2009). Standard curves were plotted to determine genome levels using synthesized human norovirus (GII.4 Sydney) 10-fold RNA dilutions.

Murine Norovirus

Murine norovirus was quantitated according to Levenson et al. using Ag-Path-ID 1 Step RT-QPCR Master Mix (Thermo Fisher Scientific, Waltham, MA) and ORF1 specific forward primer 5′-GGCTACGGCTGGACATGTCT, reverse primer 5′-GCGTCAGGCC TATCCTCCTT, and 6-FAM-BHQ1 labeled probe 5′CTATCTTCCGCCGTTACCCCCATCTG (LGC Biosearch Technologies, Petaluma, CA). The qPCR reaction conditions were prepared following manufacturer's recommendation and run in triplicate on the Applied Biosystems 7900 HT instrument. RTS/Genomics used 100 nucleotide synthetic DNA encompassing ORF1 PCR amplicon (5′-TCTGATCCGTGGCTACGGCTGGACATGTCTGATAAGGCTATCTTCCGCCGTTACCCCCATCTGCGGCCTAAGGAGGATAGGC CTGACGCGCCCTCCCATG) from Biosearch Technologies (Petaluma, CA) was used for the viral copy standard. Viral copy number was calculated using the standard curve method according to the manufacturer's protocol (Life Technologies, Carlsbad, CA).

Human Rotavirus

Human rotavirus RNA was extracted using MagMax-96 Viral Isolation kit from 200 μl of each sample according to the manufacturer's recommendations. The extracted RNA was stored at –70°C until testing. RT-PCR was used for the detection of RVA RNA by using primers NSP3F and NSP3R and a QuantiTect SYBR green RT-PCR kit. The following conditions were applied: incubation for 20 min at 50°C for the reverse transcription reaction and a preheating step at 95°C for 15 min for initial denaturation, followed by 40 PCR cycles at 94°C for 15 s, 56°C for 30 s, and 72°C for 30 s. A melting-curve analysis was then performed at 95°C for 5 s and at 65°C for 1 min, slowly increasing the temperatures up to 97°C for over 20 min, followed by a 40°C hold. RNA extracted from a validated RVA-positive sample was used as a positive control, while RNA-free water was used as a negative control (Shao et al., 2015).

CD300fL Antibody Treatment

Cell Infectivity

RAW264.7 cells in 24-well plates (seeded at 5×10^4 cells per well and incubated for 24hr) were pre-treated with 500ng anti-CD300fL or IgG antibodies per well. For replication analysis, cell cultures were inoculated with either virus vesicles or free virus and incubated at 37°C/5%CO_2 for the required time. Finally, cells were rinsed with 1xPBS and lysed using cell lysis buffer supplemented with protease and phosphatase inhibitors. Lysates were centrifuged and supernatants were stored at -20°C until further processing.

Labeled Vesicles

RAW264.7 cells were seeded in coverslips after a 30-minute pre-treatment with either anti-CD300fL or IgG antibodies. Subsequently cells were inoculated with CellBrite488 labeled vesicles and further incubated for 30 minutes at 37°C/5%CO_2. Finally samples were rinsed, fixed, and mounted. Z-stack images of fixed cells inoculated with labeled vesicles, were examined as follows: Green fluorescent vesicles were marked with circles on each slice of the Z-plane. The total number of vesicles was tallied and divided by the total number of cells in the field of view. An average ratio of associated vesicles to cells was calculated for both mock-IgG and anti-CD300lf treated cells. Two stacks with 25 sections of 0.44 nm thickness with an average of 75 cells per field view were analyzed per treatment group.

GW4869 Treatment

RAW264.7 cells were pre-treated for 12hr with 10μM GW4869 or DMSO. GW4869 was prepared to 2μM stock in DMSO and further diluted to working concentration in culture media depleted of extracellular vesicles by centrifugation at 100000 x g. Then, cultures were inoculated with virus stock and incubated for 1hr at 37°C/5% CO_2. Later, cultures were rinsed with pre-warmed SFM and further incubated in exosome depleted cell culture media supplemented with GW4869 or DMSO for the required time frame. Culture media was collected to isolate vesicles. Finally, cells were rinsed with 1xPBS and lysed using cell lysis buffer supplemented with protease and phosphatase inhibitors. Lysates were centrifuged and supernatants were stored at -20°C until further processing.

Electron Microscopy

Whole Mount

Isolated vesicles were mounted on 400 mesh carbon coated copper grids (EMS, PA) (grids were glow discharged for 1minute) and incubated for 15 to 30 minutes in a humidifying chamber at RT; then sample grids were placed in fixative (4% PFA, 0.1% Glut, in 1xPHEM buffer pH6.9) and incubated for 10 minutes at RT, followed by 3 spot rinses in 1xPBS and 2 in ultrapure water. Fixed sample grids were spot stained with aqueous 0.5% w/v uranyl acetate solution or NanoVan for 1 minute at RT and blot dried.

Transmission Electron Microscopy

Samples were fixed for 1hr with 2.5% glutaraldehyde and 1% formaldehyde in 0.12 M sodium cacodylate buffer, pH7.4. Samples were post fixed in 1% osmium tetroxide in cacodylate buffer, *en bloc* stained with 1% uranyl acetate, dehydrated in an ethanol series/propylene oxide and embedded in EMbed 812 resin (EMS, PA). Ultra-thin sections (50-60 nm) were obtained using and EM UC7 ultramicrotome (Leica, Vienna, Austria). Images were acquired at the NHLBI electron microscopy core facility using the JEM 1200EX (JEOL USA) transmission electron microscope (accelerating voltage 80 keV) equipped with and AMT 6-megapixel digital camera (Advanced Microscopy Techniques).

Immuno-Labeling

Sections were loaded on grids, as described above, and spot rinsed 3 times 2 minutes each with 1x PBS. Samples were incubated for 20 minutes in blocking buffer (0.15% Glycine in 1xPBS) and spot rinsed 3 times 2 minutes each with 1x PBS. Following, samples were incubated with primary sheep anti-rotavirus antibodies (GTX39230, Genetex) in dilution buffer (2% BSA and 0.1% FSG in 1xPBS) for 1hr. After spot rinsing with 1xPBS samples were incubated in 6nm anti-sheep immuno gold antibody (AURION Immuno Gold Reagents and Accessories, Wageningen, Netherlands). Next, samples were spot rinsed and fixed in 1% glutaraldehyde in 1xPBS for 5 minutes. Finally, samples were spot rinsed in ddH2O 6 times 1 minute each, incubated in 1% uranyl acetate for 5 minutes and allowed to air dry. The entire procedure was carried out at room temperature.

Correlative-Light Electron Microscopy

Optical imaging of fluorescent samples was performed with LSM 780 confocal laser scanning microscope (Carl Zeiss, USA). Once confocal images were obtained, culture dishes (MatTek glass bottom, P35G-1.5-14-CGR) were fixed in 2.5% glutaraldehyde, 1% paraformaldehyde, 0.1M sodium cacodylate buffer, pH 7.4, rinsed in cacodylate buffer, post fixed with 1% OsO_4 in the same buffer, and dehydrated in an ethanol series. The coverslips were removed from the dish, dried using a Samdri-795 critical point dryer (Tousimis Research, Rockville MD), coated with 5 nm gold in an EMS 575-X sputter coater (Electron Microscopy Sciences, Hatfield PA) and imaged with a Zeiss Crossbeam 540 (ZEISS, Jena Germany). Alignment of light and scanning electron microscopy images was done with the eC-CLEM plugin. Firstly, the LM image was aligned based on manually inserted landmarks. After this coarse alignment, a finer alignment was performed by registering the center of several (15 to 20) clearly identified labelled structures and their corresponding signals on the SEM micrographs.

Immunoprecipitation and Co-immunoprecipitation

Antibodies against the target protein/virus were coupled to protein "A" or "G" beads with 0.5μg of antibody per 1μl of bead suspension and incubated in 1xPBST at 4°C for 30 minutes with gentle mixing, bead/antibody complex was washed 3 times with 1xPBS and then added to the cell lysates or clarified fecal/gut suspensions to further incubate at 4°C for 1 to 3 hours with gentle mixing. Bead/antibody/antigen complex was washed 3 times with 1xPBS. Finally, antibody/antigen complexes were eluted from beads by adding 2x protein loading buffer (2x laemmli buffer; 5% betamercaptoethanol) and boiling them at 95°C for 10 minutes.

SDS-PAGE and Western Blot Analysis

PAGE was carried out using 10% or gradient 4–20% TGX precast gels (BioRad, CA) at constant 200 volts and transferred to 0.2 μm nitrocellulose membranes in a Trans-Blot Turbo transfer system. Membranes were blocked for 1hr at RT in blocking media (5% NFM and 0.1% tween-20 in 1x TBS). After blocking, membranes were incubated overnight 4°C in the primary antibody solution (1% BSA, 0.02% NaN_3, 0.1% tween-20, in 1x TBS), then washed with 1x TBST 6x-10 minutes each; followed by incubation for 1hr at RT in secondary antibody diluted in blocking solution then washed with 1x TBST 6x-10 minutes each. Membranes were treated with chemiluminescent substrate (Thermo Scientific, IL) and developed using the Amersham Imager 600 (GE Healthcare Life Sciences, PA).

MALDI-TOF/MS Lipid Analysis

Analyses of Intact Viral Membrane Vesicles

Intact viral membranes were deposited on the MALDI target with a "double layer" deposition method as follows: a 1 μl droplet of the vesicle suspension, diluted in distilled water to a concentration of about 66 μg/ml, was deposited on the MALDI target and dried under a cold air stream (first layer); the resultant solid deposition was then covered by a thin second layer (0.35 μl droplet) of the 9-AA matrix solution (20 mg/ml in 2-propanol-acetonitrile, 60:40, v/v). After solvent evaporation, the sample could be analyzed.

Mass Spec Settings

MALDI-TOF mass spectra were acquired on a Bruker Microflex LRF mass spectrometer (Bruker, Germany). The system utilizes a pulsed nitrogen laser, emitting at 337 nm; the extraction voltage is 20 kV, and gated matrix suppression was applied to prevent detector saturation. The laser fluence was kept about 10% above threshold to have a good signal-to-noise ratio. All spectra were acquired in the reflector mode using delayed pulsed extraction; spectra acquired in negative and positive ion mode are shown in this study. Spectral mass resolutions and signal-to-noise ratios were determined by the software for the instrument, "Flex Analysis 3.3" (Bruker Daltonics).

QUANTIFICATION AND STATISTICAL ANALYSIS

Rotavirus Quantitation by ELISA Assay

ELISA assay was performed using EDI Fecal Rotavirus Antigen ELISA Kit according to manufacturer protocol. In summary, samples from cell culture and tissue homogenates were diluted 10 times with sample diluent buffer provided in the kit. A 100 μl aliquot of the diluted samples was added to each of the wells. For Stool samples, an equal volume of clarified stool solutions was used directly for analysis. A set of standards was included (0,1.9,5.6,16.7,50,150 and 300 ng/ml). Samples were incubated for 1 hour at room temperature (RT). Wells were washed 5 times with washing buffer; then, wells were incubated with 100 μl of tracer antibody for 30 minutes at RT. Followed by a second washing step and addition of the antibody substrate. Samples were incubated in the dark for up to 15 minutes, then 100 μl of the stop solution was added to halt the reaction. The absorbance readings (at 450 nm) were performed in the Synergy H1 microplate reader (BioTek instruments, VT). A standard curve was plotted and the concentration of the samples was calculated from the curve.

Diarrhea Scoring of Mouse Feces

Stools collected from test mouse groups every day for 7 days were stored at 4°C and analyzed for diarrhea. A scoring system was utilized in order to describe the severity of infection over the different days among the groups (Boshuizen et al., 2003). Normal dry feces were given a score of 1 and exceptionally loose feces were given a score of 4. Any score above 2 was considered as diarrhea. Loose yellow-green feces were scored as 3 and watery feces were scored as 4. A mean diarrhea score was calculated considering the independent scorings from each experiment.

Statistical Analyses

p values were determined by either unpaired Student's t test or one-way ANOVA followed by Tukey's multiple comparisons test using Graphpad Prism 7.02 Software. p values <0.05 were considered significant and denoted by *. Information about number of animals used per independent experiments is also mentioned with corresponding figure legends.